Journal of Geophysical Research: Solid Earth

RESEARCH ARTICLE 10.1002/2017JB015235

Key Points:
• The Northern Apennine thrust belt shows a thin-skinned tectonic style with two main décollements in Upper Carnian and Oligocene shaly units
• Salient and recess development is primarily controlled by lateral facies variations of the stratigraphic units hosting the décollements
• Salients are more pronounced where the flexural behavior of the Adriatic slab has induced a steeper geometry of the basal décollement

Supporting Information:
• Supporting Information S1

Correspondence to:
D. Scrocca,
davide.scrocca@igag.cnr.it

Citation:
Livani, M., Scrocca, D., Arecco, P., & Doglioni, C. (2018). Structural and stra tigraphic control on salient and recess development along a thrust belt front: The Northern Apennines (Po Plain, Italy). *Journal of Geophysical Research: Solid Earth*, *123*. https://doi.org/10.1002/ 2017JB015235

Received 14 NOV 2017
Accepted 23 MAR 2018
Accepted article online 17 APR 2018

Structural and Stratigraphic Control on Salient and Recess Development Along a Thrust Belt Front: The Northern Apennines (Po Plain, Italy)

Michele Livani[1,2], Davide Scrocca[1], Paola Arecco[3], and Carlo Doglioni[2,4]

[1]Istituto di Geologia Ambientale e Geoingegneria, Consiglio Nazionale delle Ricerche, Rome, Italy, [2]Dipartimento di Scienze della Terra, Sapienza Università di Roma, Rome, Italy, [3]GasPlus Italiana S.r.l., Fornovo Taro, Italy, [4]Istituto Nazionale di Geofisica e Vulcanologia, Rome, Italy

Abstract The external part of the Northern Apennines accretionary wedge in northern Italy is buried beneath its fast subsiding and asymmetric foreland basin in the Po Plain. It is characterized by a diffused noncylindrical geometry resulting in salients and recesses in the study area, namely, the Cremona salient, the Parma recess, and the Ferrara salient. The interpretation of borehole and seismic reflection data suggests that the thrust belt is characterized by thin-skinned tectonic style. Two main décollement levels have been identified: a basal décollement located in the Upper Carnian units (San Giovanni Bianco Clay and Raibl Group) and a shallow décollement located in the late Eocene-Oligocene formations (Gallare Marls). The décollement surfaces dip SSW toward the hinterland of the accretionary prism, parallel to the steep (>10°) regional monocline. The geometry of the seismically active Northern Apennines system of salients and recesses is essentially controlled by the interplay of two factors: (i) the lateral facies variations of the stratigraphic units hosting and controlling the location and depth of the décollement levels and (ii) the slope of the basal décollement. Salients occur where, due to the inherited variable stratigraphy of the Mesozoic-Cenozoic Tethyan passive margin, the shaly formations hosting the two décollements are well developed allowing larger forward propagation of the thrust wedge. Recesses are instead associated to erosional-nondepositional areas. Moreover, salients are more pronounced where the flexural behavior of the Adriatic subducting slab has generated a steeper geometry of the foreland monocline and consequently of the basal décollement.

1. Introduction

Since the nineteenth century geologists studied curved thrust belts in order to understand how and why they originate (e.g., Argand, 1924; Carey, 1955; Dana, 1866; Lake, 1931; Rogers, 1858). Orogenic arcs are made up by more advanced segments (salients) separated by less advanced zones (recesses) (Miser, 1932). Within sali ents, the critical taper is lower, the distance among thrust ramps is larger, and there may be more ramps departing from the basal décollement layer with respect to the recess areas. In some instances, recesses may even be characterized by no décollement and basement-involved shortening (Boyer, 1995; Doglioni & Prosser, 1997; Mariotti & Doglioni, 2000; Mitra, 1997). Well-known examples of salient-recess systems include, among many others, the Western Alps (Argand, 1916; Lickorish et al., 2002), Jura Mountains (Hindle & Burkhard, 1999; Homberg et al., 1999; Laubscher, 1972), Taiwan (Lacombe et al., 2003; Mouthereau et al., 2002), Zagros (Allen & Talebian, 2011; Malekzade et al., 2016; Talbot & Alavi, 1996), and Sevier thrust belts (Dixon, 1982; Yonkee & Weil, 2010).

In the last decades, several explanations have been proposed about the origin of arcuate belts and salient recess systems (Ferrill

& Groshong, 1993; Hindle & Burkhard, 1999; Macedo & Marshak, 1999; Marshak, 1988, 2004; Mitra, 1997; Ries & Shackleton, 1976; Sacchi & Cadoppi, 1988; Weil & Sussman, 2004; Yonkee & Weil, 2010). Three main conceptual types of orogenic arc have been identified based on the possible strain patterns and displacement vector fields: (i) primary arcs, (ii) progressive arcs, and (iii) oroclines (e.g., Argand, 1924; Carey, 1955; Hindle & Burkhard, 1999; Merle, 1989; Weil & Sussman, 2004; Yonkee & Weil, 2010). Primary arcs develop when the arcuate shape is acquired during the initial growth of the belt and without significant increase during the following deformation stages. Progressive arcs are associated with an increasing curvature throughout the tectonic evolution of the thrust belt both caused by radially divergent slip direction and by parallel slip during differential shortening. Oroclines are due to superimposed bending, or wrenching, of a preexisting originally straight orogeny.

Journal of Geophysical Research: Solid Earth 10.1002/2017JB015235

These different types of arcuate belt may originate in response to several possible controlling factors such as (a) action of a hinterland indenter, (b) interaction of the advancing thrust belt with foreland obstacles, (c) superposed deformation, (d) stratigraphic changes in the predeformational basin fill, and (e) strength variation along the décollement surfaces (Ferrill & Groshong, 1993; Macedo & Marshak, 1999; Weil & Sussman, 2004).

Although it is quite clear that a single model or parameter cannot explain all the different curved thrust-belts, the majority of them are likely controlled by anisotropies of the predeformational tectono-stratigraphic archi tecture (i.e., basin-controlled salients in the sense of Macedo & Marshak, 1999). In particular, during the foreland-ward propagation of the thrust belt, the structural setting of the preexisting domains, together with the mechanical properties of the associated geological units, plays a key role in determining along-strike changes of the following relevant parameters (e.g., Aitken & Long, 1978; Boyer, 1995; Davis & Engelder, 1985; Davis, Suppe, & Dahlen, 1983; Lenci & Doglioni, 2007; Macedo & Marshak, 1999; Marshak, 2004; Mitra, 1997): (i) internal strength of the thrust wedge (e.g., the Sevier fold-thrust belt in Utah; Mitra, 1997); (ii) geo metry and depth of the décollement levels (alias detachments), including basement involvement and lateral changes from thin-skinned to thick-skinned style of deformation (such as in Taiwan; Lacombe et al., 2003; Mouthereau et al., 2002); and (iii) friction on the décollement layers (e.g., the Sulaiman salient in Pakistan; Davis & Lillie, 1994). As an example, a thick basin sequence hosted in a graben may favor the propagation of the thrust belt and the formation of a salient due to the presence of weak rocks within the thrust wedge or the presence of a more efficient basal décollement (e.g., Butler et al., 1987; Davis & Engelder, 1985). Moreover, the deeper the décollement, the larger the volume of rocks involved in the accretionary prism, as documented for instances in the Apennines fold and thrust belt (Bigi et al., 2003; Lenci et al., 2004).

Steeper regional monoclines, which may also be controlled by a higher amount of flexural subsidence of the subducting lithosphere, promote the movement of thrust belts and the consequent development of salients. Conversely, less steep regional monoclines inhibit their advancement and induce the formation of recesses (for instance, the Sevier fold-thrust belt in Utah; Boyer, 1995; Mitra, 1997, and the Apennines thrust belt; Mariotti & Doglioni, 2000). Finally, the presence of volcanic edifices (such as seamounts or volcanic ridges) on the subducting plate can influence salient and recess development as observed along numerous active margins (see, for instance, Dominguez, Malavieille, & Lallemand, 2000; Dominguez et al., 1998).

To contribute to the understanding of how these different factors can interact in shaping the salient-recess pattern, in this paper, we investigate one noticeable example of a curved thrust belt represented by the Northern Apennines in Italy. Based on borehole and seismic reflection data, we report a structural analysis of the northern segment of the Northern Apennines accretionary prism front (Figure 1), which is buried along the southern side of the Po Basin (northern Italy). The Po Basin is a Plio-Pleistocene asymmetric subsiding foreland basin resulting from the north-eastward retreating Adriatic continental subduction zone.

The Northern Apennines buried front has been very well defined since the 1980s by the interpretation of seis mic reflection profiles (Fantoni & Franciosi, 2010; Pieri, 1983; Pieri & Groppi, 1981; Turrini, Lacombe, & Roure, 2014). Three different arcs have been recognized along the thrust front: the Monferrato, the Cremona, and the Ferrara arcs (see Consiglio Nazionale delle Ricerche, 1992). The accretionary prism front is seismically active (Albano et al., 2017; Benedetti et al., 2003; Boccaletti, Corti, & Martelli, 2011; Bonini et al., 2014; DISS Working Group, 2015; Govoni et al., 2014; Lavecchia et al., 2012; Michetti et al., 2012; Toscani et al., 2009; Turrini et al., 2015; Vannoli et al., 2015, and references therein). Before the M_L 5.9, 20 May 2012 Emilia earth quake, the area was characterized by low strain rate, which potentially indicates a greater likelihood for more numerous and larger earthquakes (Cuffaro et al., 2010; Doglioni et al., 2011, 2015; Riguzzi et al., 2012).

To date, several issues are still a matter of scientific debate, such as the overall tectonic style and the connec tion modalities between the orogenic arcs and the related causative processes. The arcuate geometry of the

Northern Apennines has been alternatively interpreted as due to (i) inherited heterogeneity in the upper crust (e.g., presence of extensional paleo-domains or intrasedimentary volcanic bodies) of the subducting plate (e.g., Cassano et al., 1986; Castellarin et al., 1985; Cuffaro et al., 2010), (ii) dislocation of the thrust front by strike-slip faults (e.g., Costa, 2003), or (iii) the interplay between N-S oriented preorogenic extension related faults and about ESE-WNW oriented compressional faults (Turrini et al., 2014, 2016). Regarding its tectonic style, two conflicting hypotheses have been proposed. The first one suggests a thin-skinned style (e.g., Carminati, Cavazza, et al., 2010; Pieri & Groppi, 1981; Wilson et al., 2009), while the second one infers a thick-skinned style (e.g., Argnani et al., 2003; Artoni et al., 2007, 2010; Boccaletti et al., 2004; Capozzi &

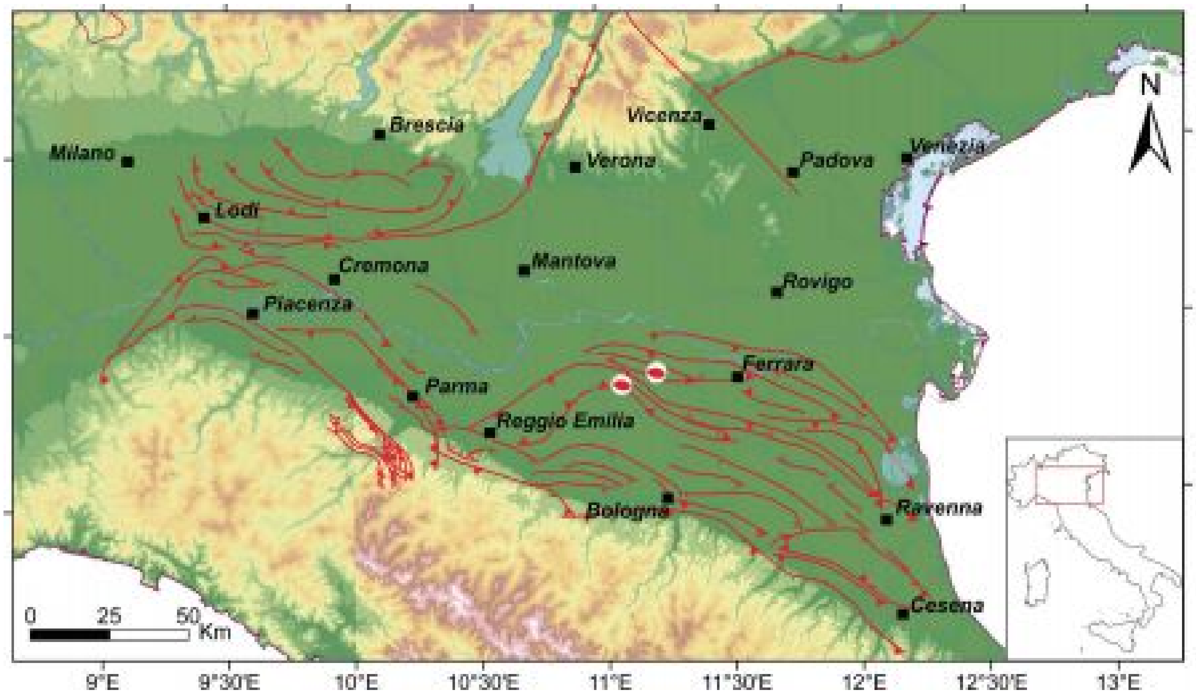

Figure 1. Study area and simplified structural map of the Po Plain. The red color indicates the main thrusts mapped in the subsurface based on our reinterpretation of the available data and critical review of already published maps and cross sections (e.g., Pieri & Groppi, 1981; Pieri, 1983; Consiglio Nazionale delle Ricerche, 1992; Boccaletti et al., 2004; Fantoni & Franciosi, 2010). Thrusts are differentiated according to their décollement level: The solid triangles indicate ramp originated from the basal décollement level located in the Upper Carnian (San Giovanni Bianco Clays and Raibl Group), while the empty triangles correspond to ramp rooted in the shallower décollement level located in the Oligocene (Gallare Marls). The dashed yellow line represents the trace of the seismic reflection profile reported in Figure 5. The blue lines correspond to chronostratigraphic charts (A-A^0 and B-B^0) in Figures 6 and 7, paleogeographic section (B-B^0) in Figure 10, and geological cross sections (C-C^0 and D-D^0) in Figure 11. The turquoise line represents the trace of the schematic geological cross section reported in Figure 3. The focal mechanisms of the main seismic events of the 2012 Emilia earthquake (M_L 5.8 and 5.9) are also located on the map (Govoni et al., 2014).

Picotti, 2009; Carannante et al., 2015; Fantoni et al., 2004; Fantoni & Franciosi, 2009, 2010; Lavecchia et al., 2012; Picotti et al., 2007; Picotti & Pazzaglia, 2008). Recently, a mixed thin-thick-skinned tectonic style has been also proposed (e.g., Turrini et al., 2016).

Our study, which has been carried out by reinterpreting existing well data, seismic reflection profiles, and published information, includes an area that extends from the Lombard plain in the West to the Adriatic coast in the East and laps the outcropping edges of the Northern Apennines in the South and of the Southern Alps in the North (Figure 1). Its purpose is to highlight new elements useful to better understand the overall tec tonic style of the Northern Apennines front and to define the different processes responsible for the genesis of its arcs, unraveling the interplay between these processes.

2. Geological Setting

The Northern Apennines thrust belt (Figure 1) developed since Neogene times in the hanging wall of a west directed subduction zone (e.g., Doglioni, 1991; Royden et al., 1987; Scrocca et al., 2007). The foreland-ward propagation of the Northern Apennines thrust system and foreland flexure (with the consequent shift of the associated foredeep basins) is controlled by the eastward retreat of the subducting Adriatic lithosphere (among many others, Carminati, Doglioni, & Scrocca, 2004; Doglioni, 1991; Faccenna et al., 2003; Malinverno & Ryan, 1986; Patacca et al., 1992; Rosenbaum et al., 2004; Royden et al., 1987; Scrocca et al., 2007, and references therein).

The Po Basin represents the foredeep, nowadays filled by Plio-Pleistocene turbidite and deltaic sequences of both the Southern Alps and the Northern Apennines (e.g., Bertello et al., 2010; Boccaletti et al., 2004; Carminati, Doglioni, & Scrocca, 2003; Castellarin et al., 1985; Doglioni, 1993; Fantoni & Franciosi, 2009, 2010; Ghielmi et al., 2010, 2013; Pieri & Groppi, 1981; Turrini et al., 2014, 2015, 2016). It is a fast-subsiding basin, with foredeep sediments syntectonically deposited both in isolated piggyback basins and in the prism foreland,

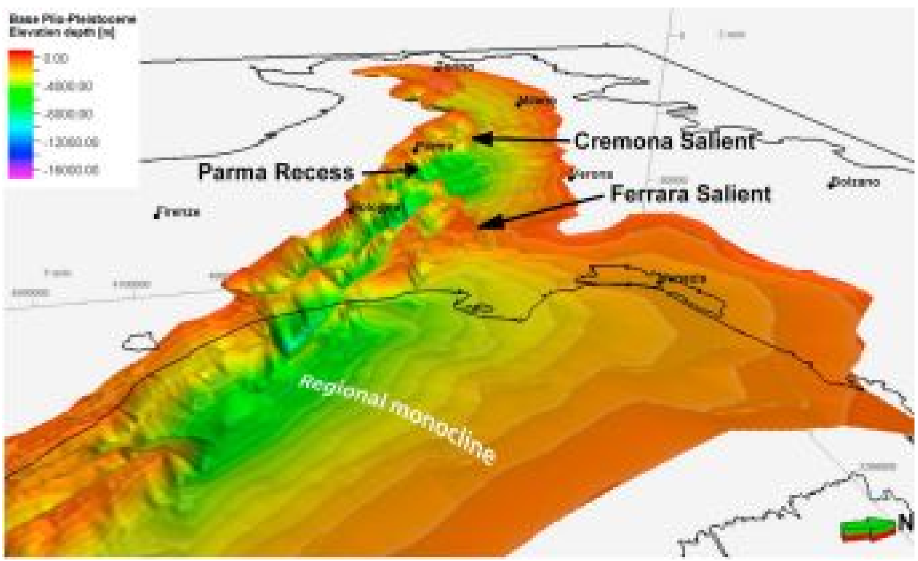

Figure 2. 3-D view of the surface that corresponds to the base of Plio-Pleistocene foredeep deposits (after Consiglio Nazionale delle Ricerche, 1992) illustrating the buried geometry of the Northern Apennines accretionary prism front. The main salients and recesses are highlighted together with the regional monocline. The green arrow indicates the north.

well described by the geometry of the base of the Plio-Pleistocene foredeep deposits shown in Figure 2 (Consiglio Nazionale delle Ricerche, 1992). This geometry is the results of the north-eastward retreat of the Adriatic slab that generated fast (>1 mm/year) subsidence on its SSW depocenter (Carminati, Doglioni, & Scrocca, 2003; Carminati & Martinelli, 2002; Turrini et al., 2016). The overall tectonic setting of the Northern Apennines and of the associated Po Basin foredeep is shown in comparison to the Southern Alps in Figure 3 (Carminati et al., 2004). The Northern Apennines accretionary prism is inferred as thin-skinned tectonics, whereas the Southern Alps are a thick-skinned thrust belt, due to their opposite polarity of subduction and to the different behavior of the subduction hinge relative to the upper plate, diverging and converging, respectively (e.g., Doglioni, 1991, 1993, 1994; Doglioni, Gueguen, et al., 1999, Doglioni, Harabaglia, et al., 1999; Doglioni & Prosser, 1997; Scrocca et al., 2007).

The belt buried beneath the foredeep sediments is characterized by a diffused noncylindrical geometry result ing in salients and recesses that are aligned in NW-SE direction (Figures 1 and 2), namely, in the study area: the Cremona salient (i.e., the Emilia Arc), the Parma recess, and the Ferrara salient (i.e., Ferrara-Romagna arc).

The Northern Apennines thrust belt has been built by off-scraping the Meso-Cenozoic sedimentary cover developed on the passive continental margin of the Adriatic plate (Figure 3), which is made up by clastics,

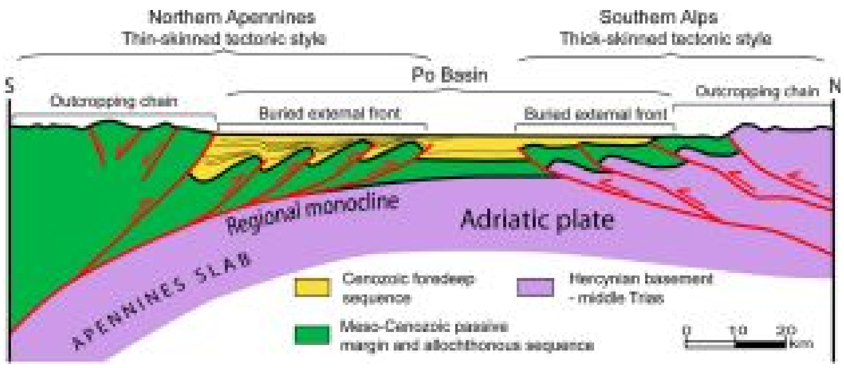

Figure 3. Schematic geological cross section that represents in a simplified form the tectonic setting of the study area (indicative section trace in Figure 1). The Northern Apennines (on the left) and Southern Alps (on the right) fronts can be identified under the Plio-Pleistocenic sedimentary cover (yellow color) that fills the Po Basin foredeep. The Northern Apennines accretionary prism is inferred as thin-skinned tectonics, whereas the Southern Alps are a thick-skinned thrust belt, due to their opposite polarity of subduction and the different behavior of the subduction hinge relative to the upper plate, diverging and converging respectively. The Apennines subduction hinge retreat subsided the Alpine front.

Journal of Geophysical Research: Solid Earth 10.1002/2017JB015235

evaporites, and shallow to deepwater carbonates (Bertotti, Picotti, & Cloetingh, 1998; Bertotti et al., 1993; Carminati, Scrocca, et al., 2010; Casero et al., 1990; Castellarin et al., 1985; Cati et al., 1987; Fantoni & Franciosi, 2010; Fantoni & Scotti, 2003; Grandić et al., 2002; Masetti et al., 2012; Turrini et al., 2014, 2016; Zappaterra, 1990). Along this passive continental margin, different Mesozoic paleogeographic domains have been identified ranging from pelagic basins to shallow water carbonate platforms.

Two conflicting hypotheses have been proposed about the tectonic style. The first one suggests that the deeper main décollement is located at the base of the Mesozoic sedimentary cover (i.e., thin-skinned tectonics; e.g., Carminati, Cavazza, et al., 2010; Cuffaro et al., 2010; Pieri & Groppi, 1981; Wilson et al., 2009), whereas the second one infers that thrusts are deeply rooted into the Paleozoic basement and the upper crust (i.e., thick-skinned tectonics; e.g., Artoni et al., 2007, 2010; Bertello et al., 2010; Boccaletti, Corti, & Martelli, 2011; Capozzi & Picotti, 2009; Fantoni & Franciosi, 2010; Fantoni et al., 2004; Picotti & Pazzaglia, 2008; Picotti et al., 2007). Recently, Turrini et al. (2014, 2016) suggested that the Plio-Pleistocene thrusting associated with the external front of the Northern Apennines also occurred with local inversion-reactivation of both flexure-related faults and pre-Alpine discontinuities. In this view, although a thin-skinned tectonic style is acknowledged as predominant, basement involvement is still considered possible.

In the study area, the 2- to 3-mm/year Global Positioning System-recorded shortening (Bennett et al., 2012; Cuffaro et al., 2010; Devoti et al., 2008) produces earthquakes that have rarely produced so far coseismic slip larger than 1 m at 6- to 10-km depth, with expected magnitude possibly slightly larger than 6 (e.g., Cuffaro et al., 2010; Grenerczy et al., 2005). Therefore, surface ruptures are rare or unlikely because shallow coseismic deformation occurs in folds above the tip line producing uplift over the main ramp and subsidence above the hypocenter, as predicted by thrust modeling (Doglioni et al., 2015) and recorded by interferometric synthetic aperture radar data of the M_L 5.9 and 5.8 Emilia 20 and 29 May 2012 seismic sequence (Galli et al., 2012; Govoni et al., 2014; Tizzani et al., 2013).

3. Data and Methodologies

This study is based on the analysis and interpretation of subsurface geophysical data, consisting of well data and seismic reflection profiles, acquired in the Po Valley for mining purposes (Figure 4). These data, in the public domain, are available on the website of the ViDEPI (Visibility of petroleum exploration data in Italy) Project carried out to make all the documents concerning Italian oil exploration easily accessible (ViDEPI Project, 2015). The available documentation concerns expired, and therefore public, mining permits and con cessions filed since 1957 by the National Mining Office for Hydrocarbon and Geothermal Energy (UNMIG), of the Italian Ministry for Economic Development. Moreover, one seismic profile has been provided by the GasPlus Italiana S.r.l. company and is displayed in Figure 5.

The analysis and interpretation of the public domain data set have been joined by a thorough literature review. Several publications contain relevant information derived from the intense and prolonged mining activity (geophysical data, seismic profiles, well data, geological cross sections, and maps), which has been integrated into our database (e.g., Bertello et al., 2010; Boccaletti et al., 2004; Casero et al., 1990; Cassano et al., 1986; Castellarin et al., 1985; Dondi & D'Andrea, 1986; Fantoni & Franciosi, 2010; Ghielmi et al., 2010; International Commission on Hydrocarbon Exploration and Seismicity in the Emilia region, 2014; Maesano et al., 2015; Maesano & D'Ambrogi, 2017; Molinari et al., 2015; Picotti et al., 2007; Pieri & Groppi, 1981; Pola et al., 2014; Rogledi, 2010; Turrini et al., 2014, 2016).

The seismic profiles were available in paper, raster, or vector (SEG-Y) format. These seismic profiles are characterized by different quality and different datum plain. The seismic quality ranges from medium to high in the Po Plain area, and from medium to low along the outcropping edge of the Northern Apennines. Their datum plains are represented by different altitude values (i.e., 0, 200, 400, and 500 m relative to sea level).

Data from 112 public wells have also been used (ViDEPI Project, 2015). Their analysis was carried out in order to reconstruct the stratigraphy and the sedimentary evolution of the area and to calibrate seismic profiles. For this purpose, two kinds of well data have been analyzed: (i) stratigraphic information made up by geological description, formation tops, and well logs reported in composite logs and (ii) velocity data.

All datum plains (both seismic profiles and well data) have been corrected and set at sea level, corresponding to the datum plain of our project.

Journal of Geophysical Research: Solid Earth 10.1002/2017JB015235

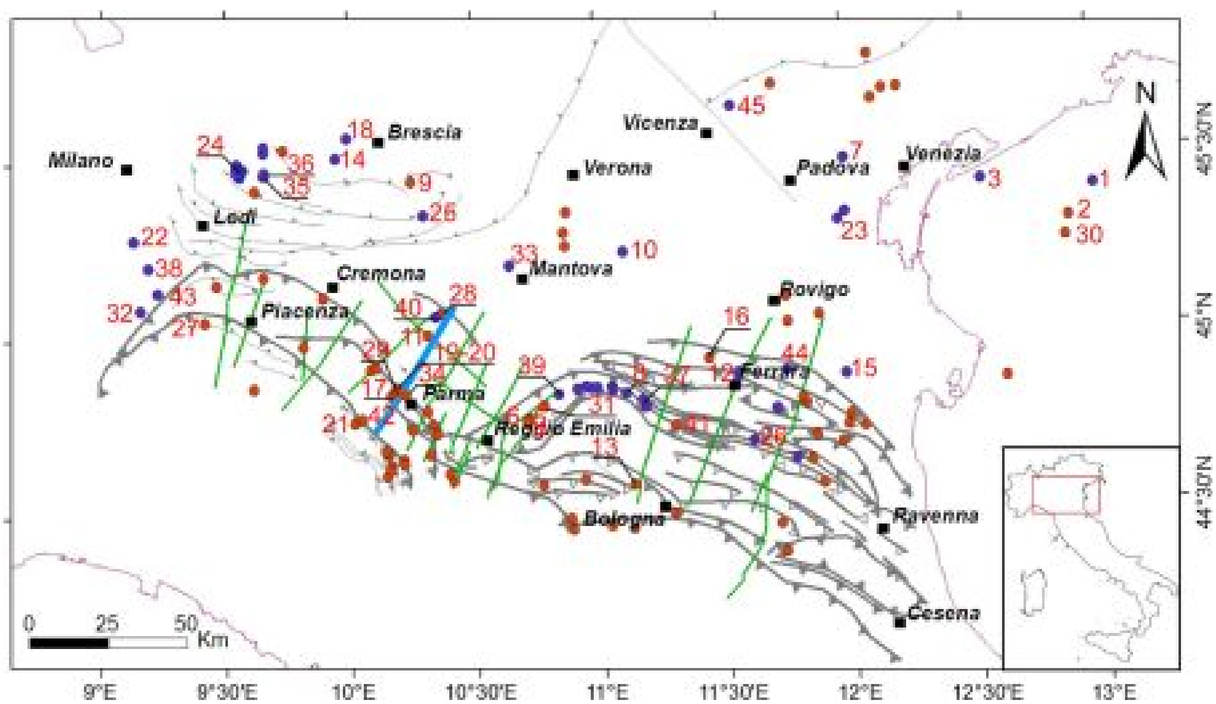

Figure 4. Map of used subsurface geophysical data showing the traces of used seismic reflection profiles, both public (green lines) (ViDEPI Project, 2015) and pub lished in this paper (blue line). Wells analyzed in this study are also shown. The brown points correspond to wells drilling only the active margin siliciclastic sequences, while the blue points represent wells drilling also the underlying passive margin units. Numbers correspond to the following wells mentioned in text or shown in other figures in this paper (in alphabetical order): Amanda 1 bis (1); Amira 1 (2); Assunta 1 (3); Bagnolo in Piano 1 (4); Bagnolo in Piano 2 (5); Bagnolo in Piano 3 (6); Ballan 1(7); Bignardi 1 and Bignardi 1 dir (8); Borgosatollo 1 (9); Bovolone 1 (10); Cantoni 1 (11); Cascina Nuova 1 dir (12); Castelfranco Emilia 3 (13); Chiari 1 (14); Corte Vittoria 1 (15); Ficarolo1 (16); Fontevivo 19 (17); Franciacorta 1 dir (18); Ghiara 1 Dir (19); Ghiara 2 dir (20); Gisolo 1 (21); Lacchiarella 1 (22); Legnaro 1 dir (23); Malossa 3 (24); Malpaga 1 (25); Marrara 1 (26); Monte Acuto 1 dir (27); Piadena 13 (28); Priorato 1 (29); Rachele 1 (30); Ravizza 1 and Ravizza 1 Or C (31); Rea 1 dir (32); Rodigo 1 (33); S. Alessandro 1 (34); S. Bartolomeo 2 (35); S. Bartolomeo 4 (36); S. Felice sul Panaro 1 (37); S. Genesio 1 (38); S. Giovanni 1 (39); Solarolo 1 (40); Spada 1 (41); Tabiano 1 (42); Valle Salimbene 1 (43); Vignola 1 (44); Villaverla 1 (45).

The few available well velocity data (e.g., ERS, 2009; ViDEPI Project, 2015) have been analyzed, and velocities for the main stratigraphic units have been calculated (instantaneous velocity for the Plio-Pleistocene deposits and interval velocities for underlying units). As an example, the time-depth chart of the Solarolo 1 well is shown in the supporting information (Figure S1). Velocity data have then been compared and integrated with information derived by previous studies (International Commission on Hydrocarbon Exploration and Seismicity in the Emilia region, 2014; Maesano & D'Ambrogi, 2017; Malagnini et al., 2012; Molinari et al., 2015; Pola et al., 2014; Turrini et al., 2014). On this base, theoretical time-depth charts have been extrapolated for wells without velocity data, but that were considered important due to their structural position or strati graphy. These time-depth charts have then been used to correlate known well tops with specific seismic hor izons interpreted on the seismic reflection profiles. Figure 5 shows an example of how well tops have been displayed on the seismic profile to constrain and identify interpreted seismic horizons.

As already discussed in previous studies (among many others, Fantoni & Franciosi, 2010; Maesano et al., 2015; Molinari et al., 2015; Turrini et al., 2014, 2016), the analysis of public well composite logs (ViDEPI Project, 2015), in addition to being important for the calibration of seismic profiles, has allowed reconstructing the stratigra phy of the study area. For this purpose, we focused our attention on two different intervals: the carbonate units (Triassic-middle Eocene), representing the passive margin sequences, and the terrigenous and siliciclas tic units (upper Eocene-Quaternary), representing the active margin sequences. From oldest to most recent the following horizons have been interpreted (Figure 5b): top Carnian, top middle Eocene (top Carbonates), top Oligocene-lower Miocene, top Langhian, top Serravallian, top Tortonian, top pre-evaporitic lower Messinian, top Upper Messinian Olistostroma, top post evaporitic Upper Messinian, top lower Pliocene, and base Pleistocene. Along the outcropping Northern Apennines edge, the top allochthonous (that coin cides with the topographic surface) has also been interpreted.

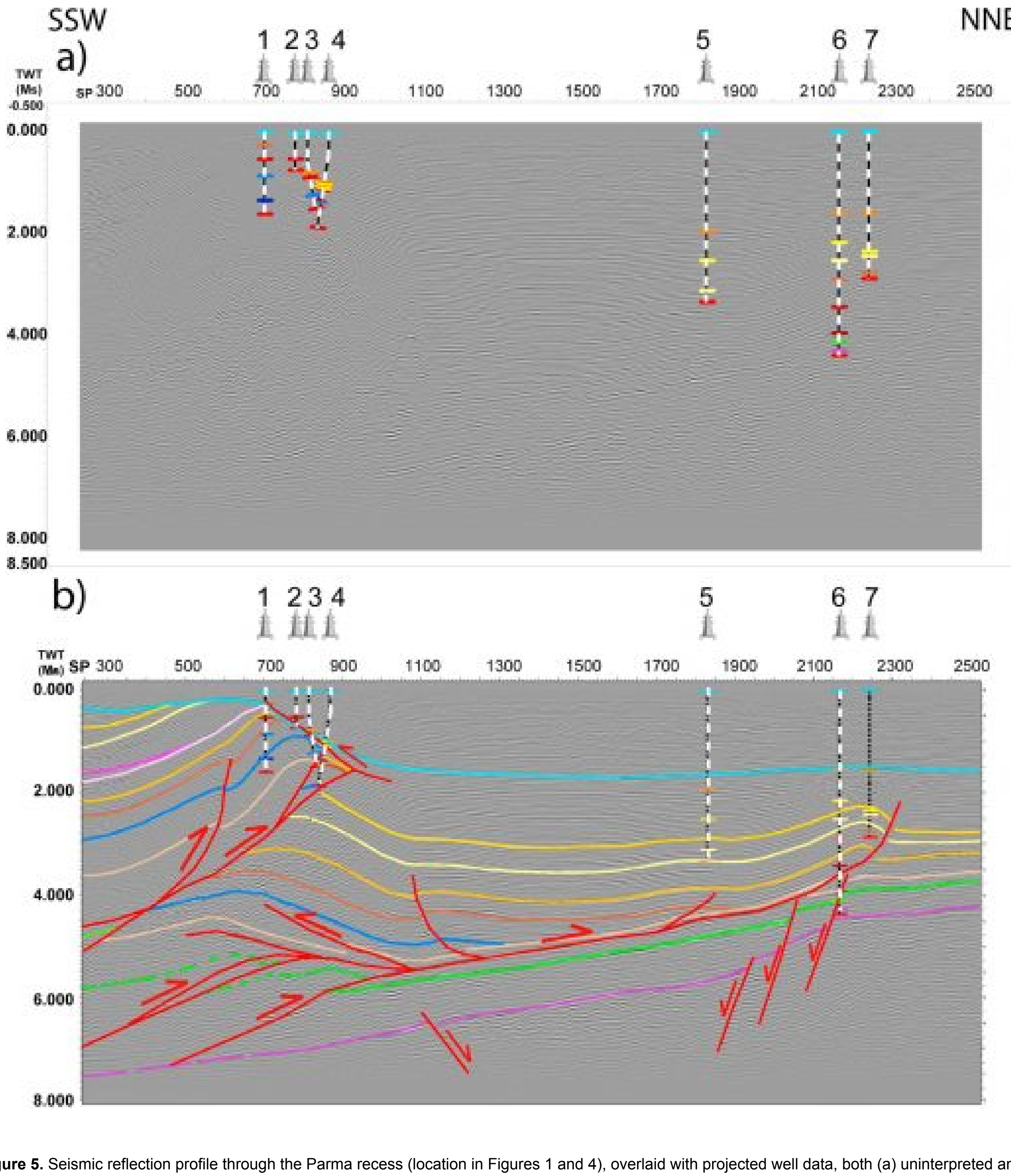

Figure 5. Seismic reflection profile through the Parma recess (location in Figures 1 and 4), overlaid with projected well data, both (a) uninterpreted and (b) inter preted. The positions of the following wells are reported: Fontevivo 19 (1); Priorato 1 (2); Ghiara2 Dir (3); Ghiara 1 Dir (4); Cantoni 1 (5); Solarolo 1 (6); Piadena 13 (7). Well paths are represented by dashed lines, while main formation tops are represented by colored hyphens. Formation tops from top to bottom: top Pleistocene (turquoise); top Upper Pliocene (Orange); top middle Pliocene (yellow); top early Pliocene (light yellow); top Messinian (brown); top Tortonian (dark brown), top Serravallian (blue); top Langhian (dark blue); top Oligocene-early Miocene (dark brown); top Eocene (green); top Liassic (violet); total depth (red). Interpreted horizon: Pleistocene base (blue), top lower Pliocene (yellow), top Messinian (light yellow), top Olistostroma (fuchsia), top preevaporitic Messinian (pink), top Tortonian (orange), top Serravallian (brown), top upper Eocene-lower Miocene (light brown), top Carbonate/middle Eocene (light green), top upper Carnian (fuchsia). Faults are shown in red.

Journal of Geophysical Research: Solid Earth 10.1002/2017JB015235

The main thrusts and faults have also been interpreted on the available seismic reflection profiles (e.g., Figure 5b). Given the presence of areas with a poor coverage of public data, the correlation of the major thrust faults interpreted on the available seismic profiles have been driven by a critical review of several published structural maps (e.g., Bertello et al., 2010; Boccaletti et al., 2004; Casero et al., 1990; Cassano et al., 1986; Castellarin et al., 1985; Consiglio Nazionale delle Ricerche, 1992; Fantoni & Franciosi, 2010; Ghielmi et al., 2010; Picotti et al., 2007; Pieri & Groppi, 1981; Rogledi, 2010). Following this approach, we have produced the structural map presented in Figure 1. Moreover, based on our reinterpretation of the available data integrated with the analysis of the published information, we have also constructed several stratigraphic charts, structural maps, and geological cross-sections.

All the available data have been elaborated in order to be managed and interpreted in digital format. As an example, paper and raster versions of the available seismic profiles have been transformed to SEG-Y format by using the IMAGE2SEGY software. Specific software solutions suitable for the integrated interpretation of seismic and well data (IHS Kingdom Seismic and Geological Interpretation Software) and for structural modeling (Move structural package) have been used.

4. Results

4.1. Stratigraphy

The analysis of well data, together with the literature review (e.g., Bertotti et al., 1993, 1998; Cassano et al., 1986; Castellarin et al., 1985; Cati et al., 1987; Dondi & D'Andrea, 1986; Dondi et al., 1982; Fantoni & Franciosi, 2010; Fantoni & Scotti, 2003; Grandić et al., 2002; Masetti et al., 2012; Pieri & Groppi, 1981; Zappaterra, 1990), has revealed that the stratigraphy of the area, from the bottom to the top, can be subdivided in three main different geological intervals:

1. metamorphic basement (pre-Permian) and overlying continental deposits (Permian),
2. passive margin mostly carbonate or marly limestone sequences (Permian-middle Eocene), and
3. active margin siliciclastic sequence (upper Eocene-present).

The Hercynian basement (pre-Permian) is overlaid by Late Permian continental (e.g., Val Gardena Sandstone) and lagoon-tidal plain sediments (e.g., Bellerophon Formation) followed by Late Permian-Triassic carbonates and marly limestones whose depositional environment ranges from lagoon-tidal plain to shallow water carbonate platform to pelagic environments (Figures 6 and 7). This sequence in some areas is characterized by the presence of intrasedimentary pyroclastic and effusive rocks of Upper Ladinian age (e.g., Ballan 1, Rodigo 1, Legnaro 1 dir, and Villaverla 1 wells), which are occasionally affected by erosive surfaces that put them in contact with the overlying Upper Triassic carbonate formations (e.g., Rodigo 1 and Ballan 1 wells).

Within the carbonate sequence, a shaly layer of regional extension has also been identified (Figures 6 and 7). It is represented by the Upper Carnian units that consist of marly dolostones and tuffaceous shales, sometimes intercalated by sulphate evaporites and volcanoclastic deposits resulting from the erosion of the Ladinian volcanic edifices (i.e., Argille di San Giovanni Bianco Fm. and Raibl Group). This level divides the Ladinian-Lower Carnian carbonates (e.g., Esino and Gorno Fm.) from the Norian ones (i.e., Dolomia Principale), except in some areas located south of Milan, north of Parma, and in the northeastern portion of the study area where the Norian dolostones overlap Ladinian-Carnian fluvio-deltaic systems (e.g., Rea 1 dir well), Ladinian volcanites (e.g., Ballan 1 and Rodigo 1 wells), and the magnetic basement (e.g., Assunta 1 well), respectively. In those areas, in fact, neritic Upper Carnian deposits are absent.

In the Upper Triassic-Jurassic interval, three different passive margin successions can be recognized in the subsurface of the Po Plain (Figures 6–10) that can be referred to three NNE-SSW oriented Mesozoic paleogeographic domains. From west to east, these paleogeographic domains, named following the terminology already proposed by Fantoni and Franciosi (2010) and Masetti et al. (2012), are as follows: (i) the Lombard Basin, (ii) the Trento Plateau, and (iii) the North Adriatic Basin (Figures 8–10). The first two (Lombard Basin and Trento Plateau) correspond to the southern prolongation of paleogeographic domains outcropping in the Southern Alps, while the last one (North Adriatic Basin) represents the western extension of the Mesozoic domain identified in the Northern Adriatic area.

The Late Triassic-Jurassic interval in the central area (Trento Plateau) is represented by a shallow water platform succession (i.e., the Upper Triassic Dolomia Principale and Lower Jurassic Calcari Grigi di Noriglio)

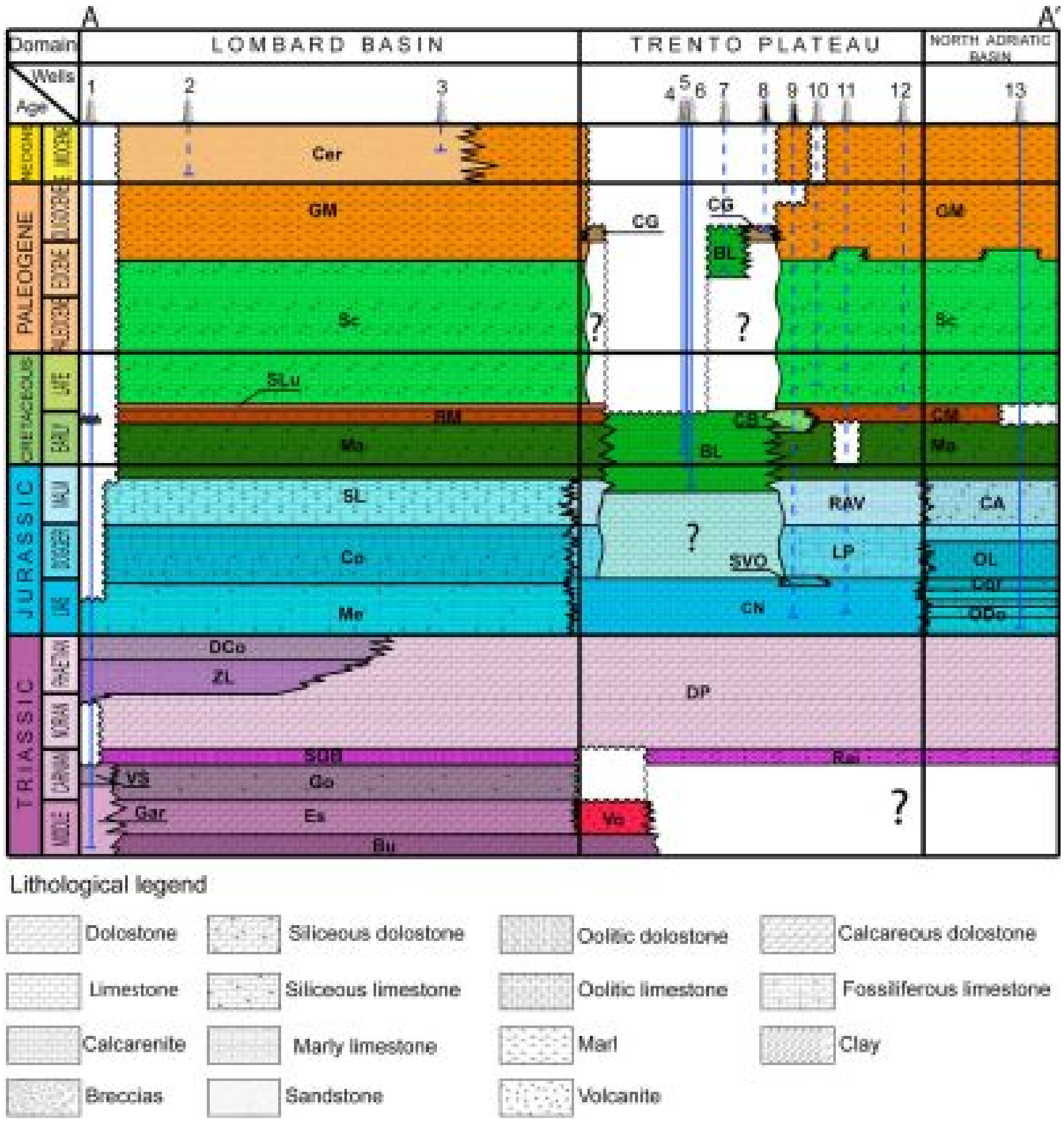

Figure 6. Chronostratigraphic chart (Middle Trias-lower Miocene age) based on well data along the transect A-A^{0}. Chart location is shown in Figures 1 and 9, while well position is specified in Figure 4. The deepest portion of the Lombard Basin is a speculative interpretation based on the stratigraphy of other wells located to the north of the chronostratigraphic section (e.g., Malossa 1 and 3, Chiari 1, and Franciacorta 1 dir), while the less constrained area below the Trento Plateau and the North Adriatic Basin is highlighted by a question mark. The following lithologies are represented (acronyms listed from older to younger and from left to right): Buchenstein Fm. (Bu); Garlasco Sandstones (Gar); Esino Fm. (Es); Volcanites (Vo); Gorno Fm. (Go); Val Sabbia Sandstones (VS); Giovanni Bianco Clays (SGB); Raibl Group (Rai); Dolomia Principale (DP); Zu Limestones (ZL); Dolomia a Conchodon Fm. (DCo); Medolo Fm. (Me); Calcari Grigi di Noriglio Fm. (CN); Soverzene Fm. (So); Igne Fm. (Ig); Corniola Fm. (Cor); San Vigilio Oolite (SVO); Concesio Fm. (Co); Fonzaso Fm. (Fo); Lumachella a Posidonia Fm. (LP); Selcifero Lombardo Fm. (SL); Rosso Ammonitico Veronese Fm. (RAV); Calcari ad Aptici Fm. (CA); Bagnolo Limestones (BL); Maiolica (Ma); Cavone Breccias (CB); Bruntino Marls (BM); Cerro Marls (CM); Marne a Fucoidi Fm. (Fm); Sasso della Luna Fm. (SLu); Scaglia Calcarea Fm. (Sc); Calcareniti di Castelgomberto (CG); Gallare Marls (GM); Gallare Marls-Gonfolite (MG-Gon); Cervarola Sandstones (Cer). The positions of the following wells are reported (from Northwest to Southesat): Rea 1 Dir (1); Monte Acuto 1 Dir (2); Gisolo 1 (3); Bagnolo in Piano 3 (4); Bagnolo in Piano 1 (5); Bagnolo in Piano 2 (6); Ravizza 1 (7); Ravizza 1 Or C (8); San Giovanni 1 (9); Bignardi 1 (10); San Felice sul Panaro 1 (11); Spada 1 (12); Marrara 1 (13).

overlaid by a drowning succession (i.e., the Middle Jurassic Lumachella a Posidonia) and a pelagic carbonate platform succession (i.e., Upper Jurassic Rosso Ammonitico Veronese) while, moving westward (Lombard Basin) and eastward (North Adriatic Basin), the transition to the basin successions occurs in the Upper Triassic and Lower Jurassic (Figures 6 and 7), respectively.

The Tithonian-middle Eocene interval is instead represented by a pelagic succession in the whole region (Figures 6–8), excluding the Bagnolo area (Figure 6), between Parma and Modena cities where the Bagnolo in Piano 1 and Bagnolo in Piano 3 wells have intercepted shallow water limestones of the Lower Cretaceous

Journal of Geophysical Research: Solid Earth 10.1002/2017JB015235

Figure 7. Chronostratigraphic chart (Middle Trias-lower Miocene age) based on well data along the transect B-B^{0}. Chart location is shown in Figures 1 and 9, while well position is specified in Figure 4. The following lithologies are represented (acronyms listed from older to younger and from left to right): Buchenstein Fm. (Bu); Garlasco Sandstones (Gar); Esino Fm. (Es); Volcanites (Vo); Gorno Fm. (Go); Val Sabbia Sandstones (VS); Giovanni Bianco Clays (SGB); Raibl Group (Rai); Dolomia Principale (DP); Zu Limestones (ZL); Dolomia a Conchodon Fm. (DCo); Medolo Fm. (Me); Calcari Grigi di Noriglio Fm. (CN); Oolitic Dolostone (ODo); Corniola Fm. (Cor); San Vigilio Oolite (SVO); Concesio Fm. (Co); Oolitic limestone (OL); Lumachella a Posidonia Fm. (LP); Selcifero Lombardo Fm. (SL); Rosso Ammonitico Veronese Fm. (RAV); Calcari ad Aptici Fm. (CA); Bagnolo Limestones (BL); Maiolica (Ma); Cavone Breccias (CB); Bruntino Marls (BM); Cerro Marls (CM); Sasso della Luna Fm. (SLu); Scaglia Calcarea Fm. (Sc); Gallare Marls (GM); Glauconie di Cavanella (GC). The positions of the following wells are reported (from Northwest to Southesat): Malossa 3 (1); Malossa 2 (2); Vailate 1 (3); San Bartolomeo 1, 2 and 4 (4); Martinengo 1 (5); Chiari 1 (6); Malpaga1 (7); Rodigo 1 (8); Villafranca 1 (9); Grezzano 1 (10); Nogarole Rocca 1 (11); Bovolone 1 (12); Ficarolo 1 (13); Cascina Nuova 1 Dir (14); Vignola 1 (15); Villadose 1 (16); Cascina Bruzzoni 1 (17); Corte Vittoria 1 (18).

(i.e., Bagnolo Limestones) overlapped by the Miocene siliciclastic formations (i.e., Marnoso Arenacea). In the same area, the Ravizza 1 well intercepts shallow water limestones of Eocene-Oligocene age overlapped by Messinian marls. In front of the Bagnolo platform some wells have drilled limestone breccias of the Upper Cretaceous (i.e., Cavone Breccias and San Giovanni 1 well).

The active margin sequence consists of an upper Eocene to present siliciclastic succession that fills the Northern Apennines and Southern Alps foredeep (Figure 8). It is made of two main depositional cycles: a lower cycle (upper Eocene-Lower Messinian) with a mostly silty and shaly component and an upper one (Upper Messinian to present) with a mostly sandy and conglomeratic clastic component (Ricci Lucchi,

Journal of Geophysical Research: Solid Earth 10.1002/2017JB015235

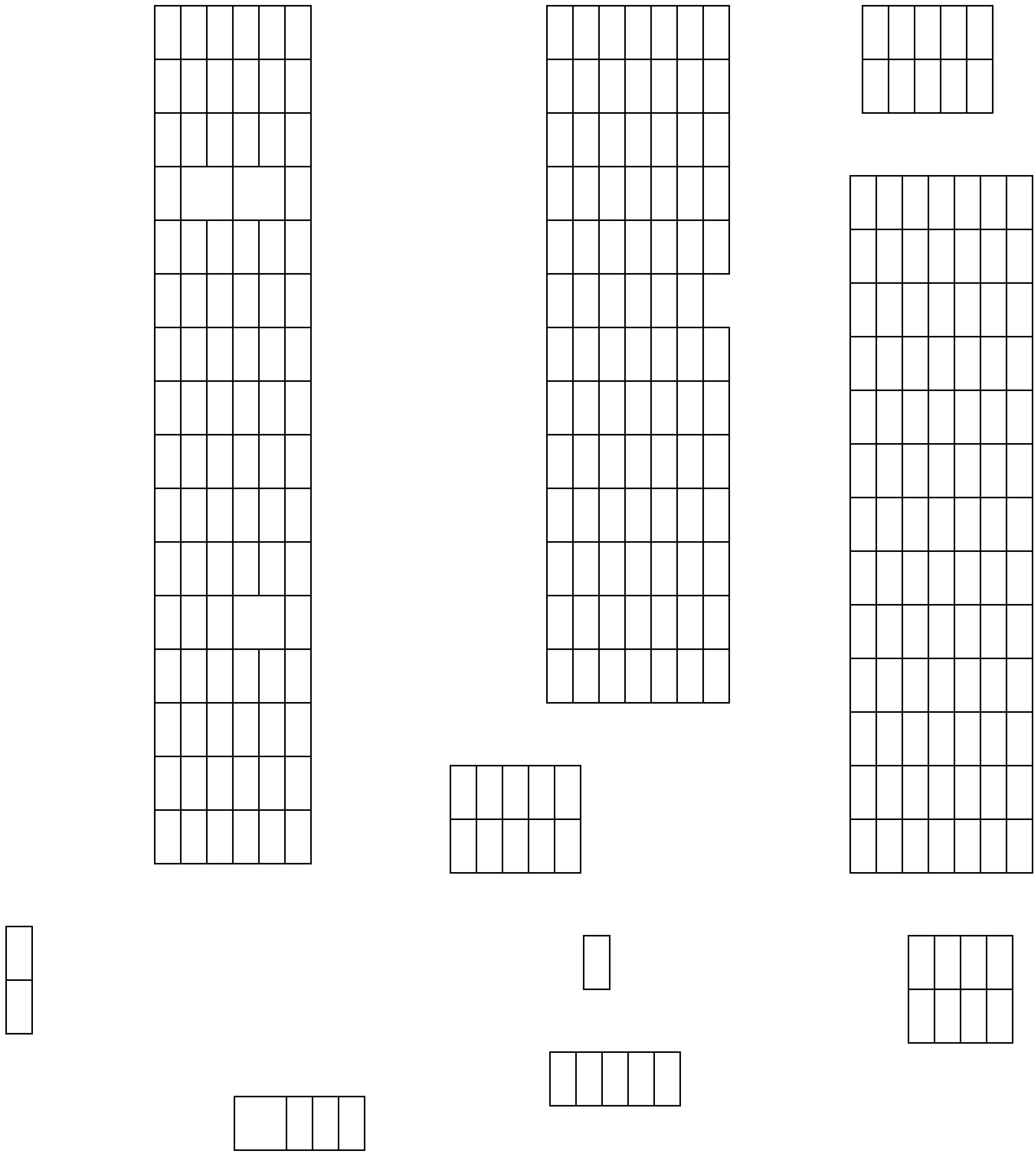

Figure 8. Synthetic stratigraphic columns of the three main paleo-geographic domains. From left to right are the Lombard Basin, the Trento Plateau and the North Adriatic Basin. The carbonate and siliciclastic sequences are distinguished (from violet to green and from brown to light yellow) and the main décollement levels are highlighted (red for basal décollement and orange for shallow décollement). The stratigraphic column to the left shows the different filling and the different for mation thickness of the Southern Alps and Northern Apennines foredeep. In the middle column we can observe the absence of the Northern Apennines décollement levels that are instead present in the left and right columns.

1986). Its basal part consists in the distal portions of foredeep filling turbidites, passing upward to proximal and more internal continental facies. This sequence is characterized by thickness and lithology variations (e.g., Gallare Marls versus Gonfolite Lombard Group) due to the tectonic and sedimentary evolution of the foredeep and of the two related chains (see Ghielmi et al., 2010). Within the active margin sequence, the Gallare Marls represent another shaly interval of regional relevance.

4.2. Structural Setting

The interpretation of the seismic reflection profiles and the study of the well log stratigraphy have revealed the interference of two types of tectonic structures in the analyzed area: the oldest and deepest type, repre sented by passive margin structures (Triassic-Jurassic in age), and the younger structures, associated with the development of the active margin involving the Miocene-Pleistocene stratigraphic terms, which in some cases reactivate preexisting faults (see also Fantoni & Franciosi, 2010; Turrini et al., 2014, 2016).

The first type of structures consists of Mesozoic horsts and grabens generated by NNE-SSW oriented normal fault systems that dislocate the Triassic-Jurassic deposits (Figures 10 and 11). The Trento Plateau is a Permian to Jurassic horst located in the central portion of the study area. It is bordered on the west and on the east by two tectonic steps that delimit it by the Lombard and the North Adriatic Basins (Figure 10), respectively. The Lombard Basin is the oldest and deepest paleogeographic domain in the study area; it is a deep structural depression divided into two main depocenters by an intrabasin horst, NNE-SSW trending and located NE of the city of Lodi beneath the S. Bartolomeo 4 well (Figures 9 and 10). The two depocenters are always NNE-SSW oriented (Figure 9), being the eastern depocenter located along the Piacenza-Brescia alignment the deeper of the two (Figure 11). The North Adriatic basin has a narrow depocentral zone that is located just east of the Ferrara-Rovigo alignment (Figure 9).

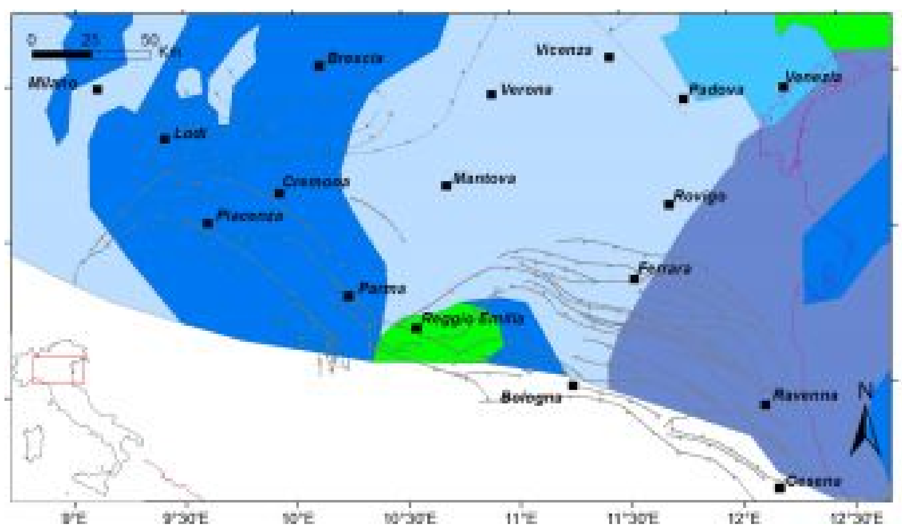

Figure 9. Map of the Mesozoic paleogeographic-tectonic domains (modified after Franciosi & Vignolo, 2002; Picotti et al., 2007; Fantoni & Franciosi, 2010; and Turrini et al., 2016). In grey, main thrusts (based on our study and literature data) differentiated on the basis of the décollement level (Upper Carnian with solid triangles; Oligocene with empty triangles). Names of the different paleogeographic domains are in red, while different orogenic sectors are in brown. The A-A^0 and B-B^0 lines represent the trace of the chronostratigraphic charts shown respectively in Figures 6 and 7; the C-C^0 and D-D^0 lines represent the trace of the geological cross sections reported in Figure 11.

The second type of structures is represented by Miocene to present folds and thrusts generated during the devel opment of the Northern Apennines. A structural map of the entire area (Figure 1) has been constructed based on the interpretation of seismic profiles and a review of published maps (e.g., Boccaletti et al., 2004; Fantoni & Franciosi, 2010; Ghielmi et al., 2010; Pieri & Groppi, 1981; Turrini et al., 2014, 2016). The main thrust structures have been identified in the southern part of the investigated area and over the passive margin structure (Figure 9).

To properly define the structural setting in the study area, two geological cross sections have been drawn based on the integrated interpretation of the available seismic and well data: one in the eastern side of the Cremona Arc and the other in the western side of the Ferrara salient (Figure 11). Interpreted faults and horizons in time domain have been first exported from the interpretation software and then uploaded into the structural modeling software. These data have been depth converted, using the available constraints for the velocity field, and then modeled to obtain the final cross sections. The structural setting shows several NNE verging asymmetric anticlines associated with SSW dipping thrust ramps converging into the décollement planes. Some back thrusts generated triangle zones. The thrust-top basins interposed between the anticlines have been filled by Neogene-Quaternary sediments. Syntectonic sedimentary wedges pinch ing out toward the anticline hinges characterize the fold limbs supporting their growth nature. The average dip angles of thrust surfaces increase toward the hinterland, in response to the progressively steeper dip of the regional monocline. However, changes of the dip angle are observed also along the same fault surfaces. They, in fact, are characterized by ramps and flats (Figure 11).

The Northern Apennines front is characterized by evident undulations (Figures 1 and 9). The most advanced portions of the thrust front (salients) are separated by less advanced segments (recesses). In the study area two orogenic arcs have been identified: the Cremona and Ferrara salients. They are divided by the Parma recess, north of the city of Parma.

The Cremona salient developed in correspondence with the Lombard Basin (Figure 9) and is composed of three main trends. From southwest to northeast they are the Salsomaggiore, the Fontevivo-Collecchio, and the Piadena anticlines (Figure 11, C-C^0). The Ferrara salient, instead, is located astride the Trento Plateau and the North Adriatic Basin (Figure 9). It involves the eastern part of the Trento Plateau, and its apex is located in correspondence with the eastern border of the plateau (Figure 9). The Ferrara arc consists of

Figure 10. Paleostructural section of the Late Jurassic through the study area with the three main tectonic domains, i.e., from west to east: Lombard Basin, Trento Plateau, and North Adriatic Basin. Location in Figures 1 and 9. Well location in Figure 4. In the middle domain, within the Triassic carbonate sequence, an intrase dimentary volcanic body (Upper Ladinian) hinders the deposition of the layer acting during the Neogene contractional deformation as a basal décollement level (Upper Carnian units in yellow, not to scale).

three main trends, which from southwest to northeast are represented by the Mirandola, Ferrara, and outer anticlines (Figure 11, D-D^0). The Parma recess occurs between the Cremona and Ferrara salients and astride the western side of the Trento Plateau. It is characterized by a smaller width compared to the Trento Plateau that extends from Parma to Bologna (Figure 9). These observations reveal that although an overall relationship between the Upper Triassic-Jurassic paleogeography and the geometry of the arcs may be observed, the position of the salients and recesses do not strictly follow the boundaries between the Trento Plateau and the adjoining Lombard and North Adriatic basins.

Some previous scientific studies (e.g., Bernini & Papani, 1987; Castellarin et al., 1985) have also reported the presence of SW-NE strike-slip faults that crosscut the orogenic complex. They are often named with the names of rivers that lie above them (e.g., Taro, Enza, Secchia, and Sillaro). However, it is not easy to identify them neither on the ground nor in the geophysical data (Molli et al., 2016). Although the geophysical data interpretation did not identify strike-slip faults, it is not possible to exclude their existence. The paleo-margins inherited from the Mesozoic passive margin evolution appear to have been used as transfer zones during the evolution of the accretionary prism, hence controlling both salients and recesses (Cuffaro et al., 2010; Turrini et al., 2016), but also the location of the past and present-day hydrography. Such transfer faults may also be characterized by the coalescence of structural undulations that control river paths and delta locations at their front in the foreland basin (Lawton et al., 1994). More internally, where the accretionary prism is now under going stretching within the backarc basin extension to the southwest of the study area, grabens may also reiterate previous transfer zones (see also Molli & Meccheri, 2012, and Turrini et al., 2016, for a discussion on heritage of transfer zones during orogenic contraction in the Northern Apennines).

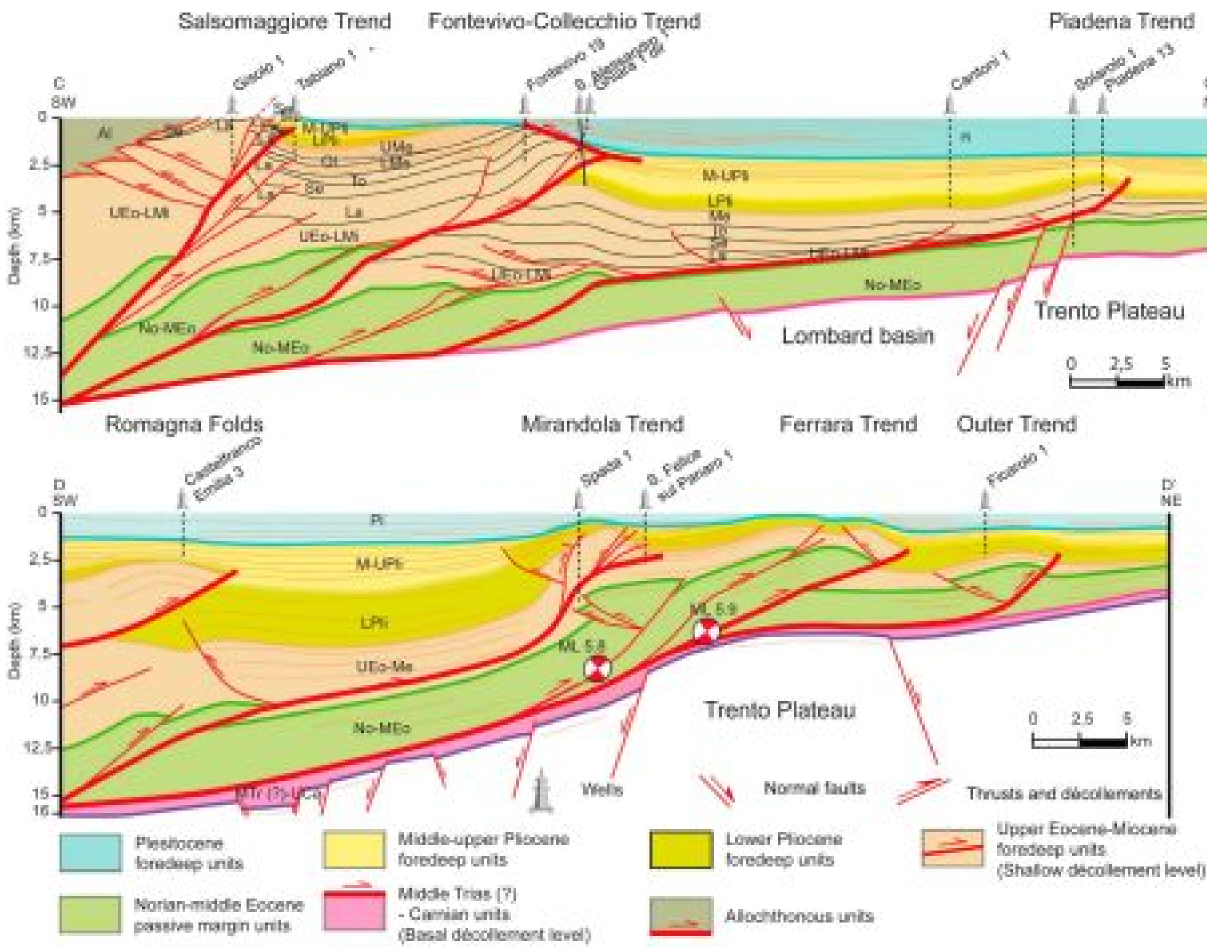

Figure 11. Geological cross-sections through the Parma recess (C-C^0) and the Ferrara salient (D-D^0). Location in Figures 1 and 9. Well location in Figure 4. Notice the in sequence propagation of thrusts toward the foreland to the right and the occurrence of several back thrusts forming triangle zones. Thrust planes are younging deeper and toward the foreland. The décollement planes are concentrated in the Upper Triassic and Oligocene layers. Note the shallower regional monocline in the upper section (C-C^0) crossing the Parma recess with respect to the steeper regional monocline in the lower section (D-D^0), crossing the Ferrara salient. The following stratigraphic intervals are shown: Middle Trias (?)-Upper Carnian (MTr-UCa); Norian-middle Eocene (No-MEo); upper Eocene-Messinian s.l. (UEo-Me); upper Eocene-lower Miocene (UEo-LMi); Langhian (La); Serravallian (Se); Tortonian (To); Messinian s.l. (Me); lower Messinian (LMe); Olistostrome (Ol); upper Messinian (Ume); lower Pliocene (LPli); middle-upper Pliocene (M-UPli); Pleistocene (Pl). The focal mechanisms of the main seismic events of the 2012 Emilia earthquake (M_L 5.8 and 5.9) are also located on the geological sections (Govoni et al., 2014). The main thrusts are highlighted (thick red lines).

Moreover, by analyzing deformations, tilting, and growth strata observed within the Miocene-Pleistocene sediments in the interpreted seismic reflection profiles and by comparing those evidences with literature data (among many others, Argnani et al., 2003; Artoni et al., 2007; Boccaletti et al., 2004; Castellarin et al., 1985; Fantoni & Franciosi, 2009; Ghielmi et al., 2010; Ori & Friend, 1984; Pieri & Groppi, 1981; Toscani et al., 2006, 2009), we have derived the timing of the first activation of the main recognized thrusts (Figure 12). Although an early activation in Messinian times of some outer thrusts in the Ferrara area has been speculatively proposed (e.g., Ford, 2004; Ori & Friend, 1984), the available constraints highlight the overall piggyback foreland propagation of the Northern Apennines thrust's imbricate fans through time (see also Ghielmi et al., 2010). Deformation is rather cylindrical during the Messinian but then thrusts propagated further within the foreland to the east (Ferrara salient) than to the west (Cremona salient).

The structural setting of the thrust system buried below the Po Plain is mainly controlled by two major décollements recognized within the Meso-Cenozoic sedimentary cover of the Adriatic plate in the Upper Oligocene to lower-middle Miocene and at the base at the Upper Triassic (Carminati, Cavazza, et al., 2010; Fantoni & Franciosi, 2010; Fantoni et al., 2004; Maesano et al., 2015; Massoli et al., 2006; Ravaglia et al., 2006; Toscani et al., 2006; Turrini et al., 2016), although other minor décollement levels may also be identified (e.g., Fantoni et al., 2004).

Journal of Geophysical Research: Solid Earth 10.1002/2017JB015235

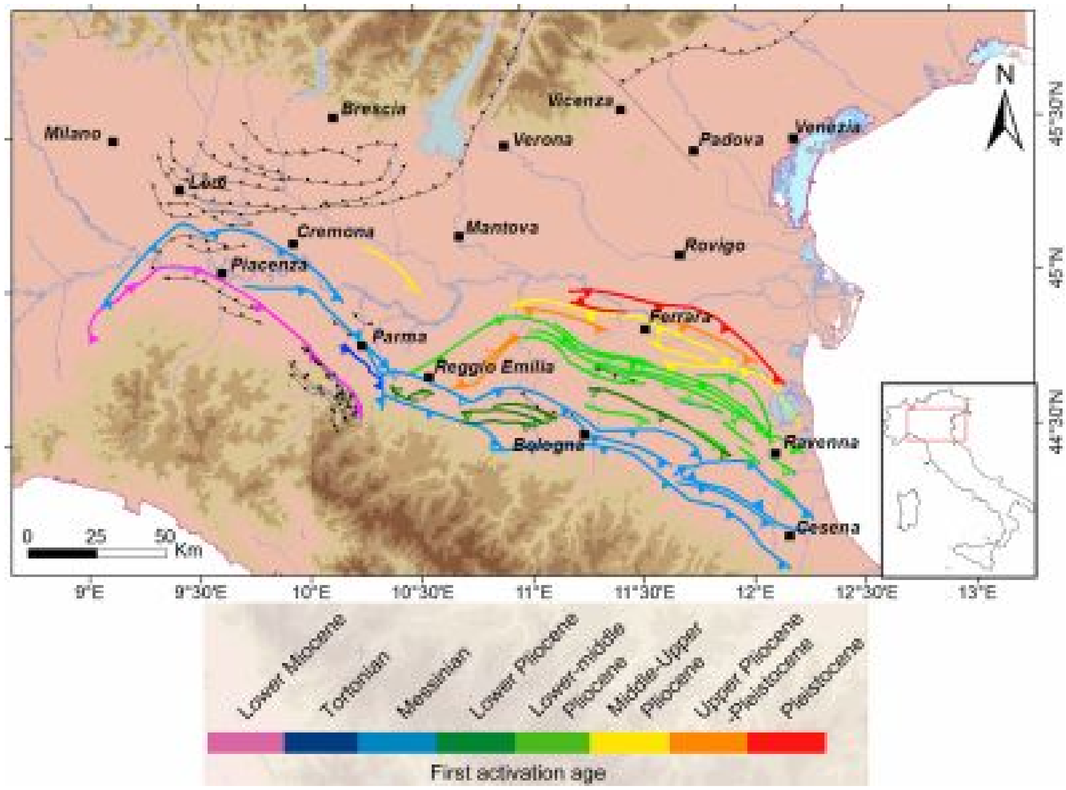

Figure 12. Structural map of the study area. Thrust ramps are in different colors according to their first activation age defined based on the deformations, tilting and growth strata observed within the Miocene-Pleistocene sediments in interpreted seismic reflection profiles compared with the literature data and structural maps (e.g., Argnani et al., 2003 ; Artoni et al., 2007 ; Boccaletti et al., 2004 ; Castellarin et al., 1985 ; Fantoni & Franciosi, 2009 ; Ghielmi et al., 2010 ; Toscani et al., 2006; Toscani et al., 2009). The chromatic variation shows the outward propagation of the Northern Apennines front through time. The solid triangles indicate ramp originated from the basal décollement level located in the Upper Carnian (San Giovanni Bianco clays and Raibl Group), while the empty triangles correspond to ramp rooted in the shallower décollement level located in the Oligocene (Gallare Marls). The C-C^0 and D-D^0 lines represent the traces of the cross-sections shown in Figure 11.

Our integrated interpretation of well and seismic data (Figure 11) shows that as discussed in detail in the following sections, these two major décollements are located in the Upper Carnian and in the late Eocene Oligocene formations in both the Cremona and Ferrara salients. Consequently, in our structural map (Figures 1, 9, and 12), thrust ramps originated from the basal décollement level located in the Upper Carnian formations (San Giovanni Bianco Clays and Raibl Group) have been differentiated by ramps rooted in the shallower décollement level in the late Eocene-Oligocene (Gallare Marls).

4.3. Upper Carnian Décollement

A decoupling of the Meso-Cenozoic passive margin cover along the Northern Apennines thrust structures bur ied below the Po-Plain is generally attributed to a basal décollement located at the bottom of the Dolomia Principale Formation within Triassic evaporites (e.g., Carminati, Cavazza, et al., 2010; Maesano et al., 2015; Massoli et al., 2006; Toscani et al., 2006). The characteristics of this regional décollement level may be obtained by the analysis of the deep wells, drilled mainly in the northern part of the study area (e.g., Corte Vittoria 1, Malossa 2, Malossa 3, and Legnaro 1 dir). These wells reveal that below the Norian-Rhaetian dolostones (i.e., Dolomia Principale Fm.), the Upper Carnian formations (Figures 6–8) consist of shales and silty dolostones with local intercalations of volcanoclastic levels, tuffaceous shales, and sulphate evaporites (i.e., Argille di San Giovanni Bianco and Raibl Group). These units, a few tens of meters thick, are bounded at the bottom by the Ladinian-Lower Carnian dolostones (i.e., Buchenstein, Esino, and Gorno formations).

As also documented by both outcrop and subsurface studies in the northern side of the study area (Laubscher, 1985; Ravaglia et al., 2006), the Upper Carnian formations represent an efficient level of regional tectonic décollement due to their shaly and silty lithology. In particular, petrophysical properties measured in outcrops in the Dolomites (Southern Alps) confirm that the Upper Carnian deposits of the Raibl Group

Journal of Geophysical Research: Solid Earth 10.1002/2017JB015235

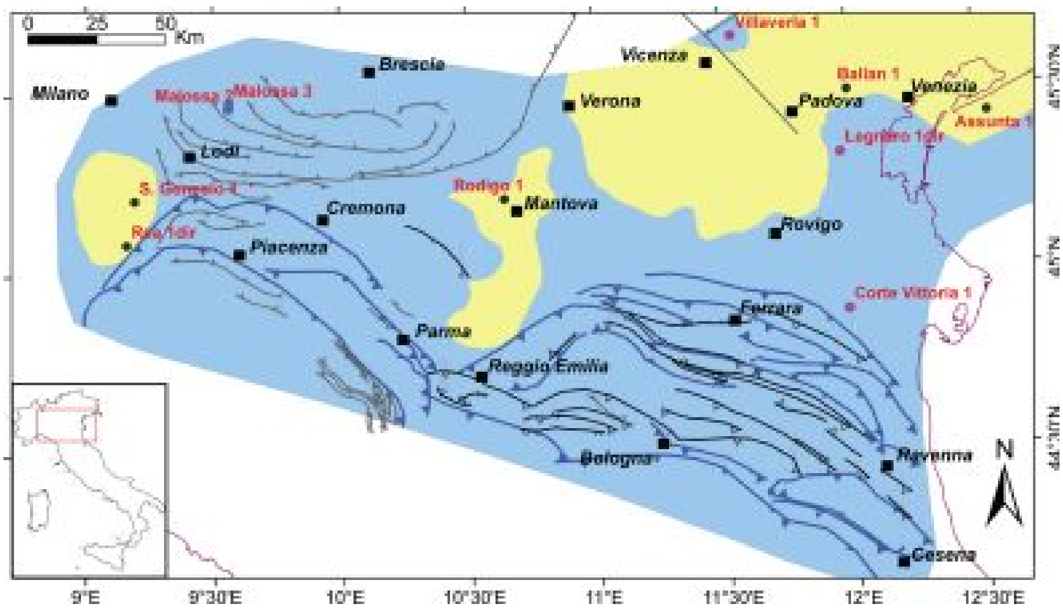

Figure 13. Map of the areal distribution of the Upper Carnian formations, corresponding to the basal décollement level, based on the analysis of well information and literature data (e.g., Cassano et al., 1986 ; Franciosi & Vignolo, 2002 ; Grandić et al., 2002). The following items are represented: depositional areas (1); erosional/ non depositional areas (the shape of the erosional/nondepositional area identified between Mantova and Parma is derived by the extent of the intrasedimentary Triassic magnetic body proposed by Cassano et al., 1986) (2); location of wells that have drilled the Upper Carnian Raibl Group (3); location of wells that have drilled the Upper Carnian San Giovanni Bianco Clays (4); location of wells without Upper Carnian units (5); thrusts rooted in Upper Carnian deep décollement (6); thrusts rooted in late Eocene-Oligocene shallow décollement (7); other thrusts (8).

represent a significant mechanical discontinuity within the Triassic carbonate succession (Rudolph et al., 1989; Stafleu & Schlager, 1993).

Based on well data, we have also identified three areas where the Upper Carnian formations hosting the regional décollement are not present (Figure 13). These areas are located south of Milan, between Mantova and Parma, and in the northeastern sector, from Verona up to the northern Adriatic where the Norian dolostones overlie Ladinian-Carnian fluvio-deltaic systems (e.g., Rea 1 dir and San Genesio 1 wells), Ladinian volcanites (e.g., Rodigo 1 well), and the Paleozoic basement (e.g., Assunta 1 well), respectively.

Because the only wells that penetrated the middle Triassic levels are essentially located in the northern portion of the study area, to tentatively map the areal distribution of the Upper Carnian formations (presented in Figure 13), the few well constraints have been integrated with other published geophysical information. The thick Ladinian volcanic units (about 575 m) drilled by the Rodigo 1 well (Figures 7 and 10), which prelude the deposition of the Upper Carnian as shown in Figure 10, are indeed associated with a clear magnetic anomaly (Cassano et al., 1986). Consequently, the shape of the erosional-nondepositional area (identified between Mantova and Parma in the map shown in Figure 13) has been tentatively derived by the extent of the intrasedimentary Triassic magnetic body proposed by Cassano et al. (1986). With a similar approach, in the northeastern sector, the areal extent of the erosional-nondepositional area has been defined by integrating the sparse well constraints with the isopach map of the Anisian-Carnian system in the northern Adriatic domain, derived by a high-quality 3-D seismic reflection survey (Franciosi & Vignolo, 2002), and with the Ladinian-Carnian paleogeographic map published by Grandić et al. (2002).

Due to the intrinsic uncertainties associated with the reconstruction of the boundaries of the Triassic magnetic body (Cassano et al., 1986) and of the Carnian paleogeographic domains (Franciosi & Vignolo, 2002; Grandić et al., 2002), the map of the areal distribution of the Upper Carnian formations (Figure 13) should be regarded as speculative. However, considering the good correspondence between the reconstructed erosional-nondepositional areas documented by a few well data and constrained by independent geophysical data sets, the correlation with the recesses deserves to be pointed out. The two erosional nondepositional areas located south of Milan and between Mantova and Parma match quite well with the

Journal of Geophysical Research: Solid Earth 10.1002/2017JB015235

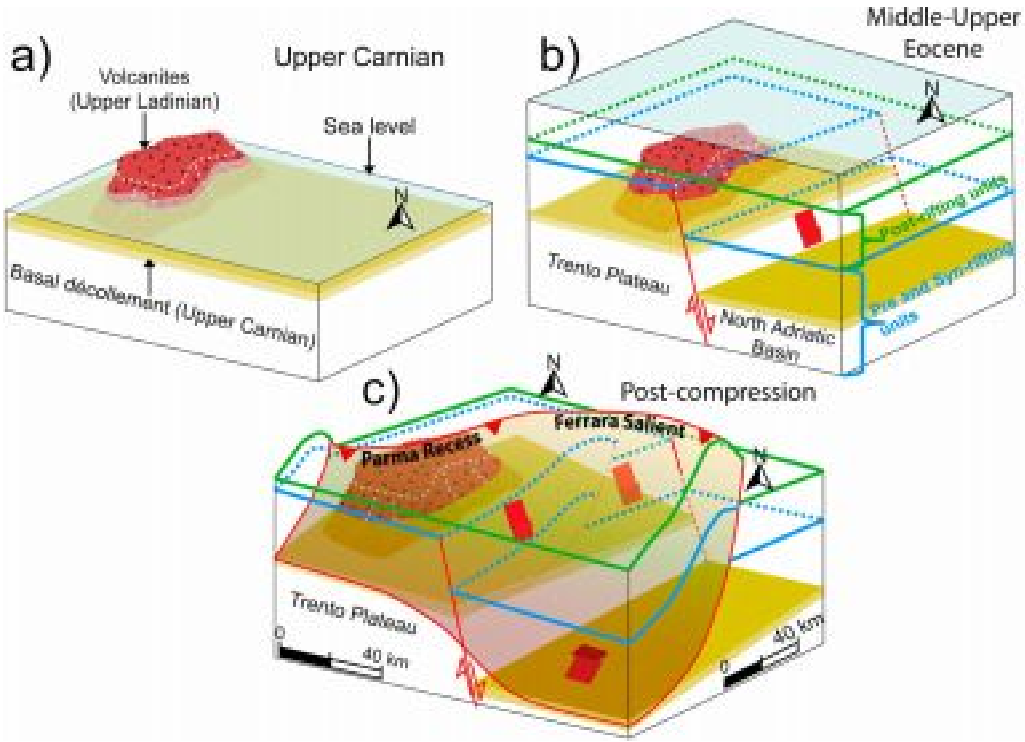

Figure 14. Conceptual model of the genesis of the Ferrara salient and Parma recess (an indicative scale is shown). (a) During the Upper Carnian age neritic clays and silty dolostones (yellow surface) deposited around Upper Ladinian volcanic edifices that emerge from the sea. (b) In the Upper Trias-Middle Jurassic age shallow water to deepwater lithologies (mainly dolostones and limestones) deposited above the Upper Carnian formations and the Upper Ladinian volcanic edifices (pre and synrifting units; top in blue color). Horst (Trento Plateau) and Graben (North Adriatic Basin) originate due to a Late Trias-Middle Jurassic extensional phase (normal fault in red). At the end, paleogeographic domains have been sutured by the Upper Jurassic-middle Eocene pelagic sedimentation (postrifting units; top in green color). (c) In this figure the interaction between the palegeographic structural setting (in figure b) and the Northern Apennines compressional phase is shown. The overlying siliciclastic deposits have been intentionally omitted for a better visibility. During thrust propagation, preexisting extensional faults are crosscut in some cases, while in other cases, they could have influenced the segmentation of the thrust fronts. The eastern side of the Trento Plateau is involved in the thrusting phenomenon, and the thrust belt front is more advanced (Ferrara salient) in areas where the basal décollement is deeper and steeper; on the contrary, it is less advanced in areas without the basal décollement (Parma recess) due to the presence of the Upper Ladinian volcanic edifices.

position of the two recesses that separate the Monferrato (located to the west and outside the investigated area) and the Cremona Salients and the Cremona and Ferrara salients, respectively (Figure 13).

A conceptual model for the deposition of the Upper Carnian deposits is illustrated in Figure 14 (see also Figure 10). During the Upper Carnian age, neritic clays and silty dolostones were deposited around the Upper Ladinian volcanic edifices. In the Upper Triassic, shallow water dolostones and limestones were depos ited above the Upper Carnian formations and the Upper Ladinian volcanic edifices. It should be noted that the differentiation between the Trento Plateau and the North Adriatic Basin, originated by a following Late Triassic-Middle Jurassic extensional tectonic phase, was not present during the Upper Carnian. This model illustrates the impact of the Upper Ladinian volcanic edifices on the genesis of the Ferrara salient and Parma recess, in analogy with the known impact on thrust front propagation of the presence on the subduct ing plate of seamounts and volcanic ridges (e.g., Dominguez et al., 1998, 2000).

4.4. Late Eocene-Oligocene Décollement

The presence of a shallower regional décollement level has been described in several previous studies. It is generally located within the upper Eocene to lower-middle Miocene Gallare Marls (Carminati, Cavazza, et al., 2010; Fantoni et al., 2004; Maesano et al., 2015; Massoli et al., 2006; Ravaglia et al., 2006, Toscani et al., 2006; Turrini et al., 2016) although an alternative position at the Top of the Scaglia Fm. has also been proposed by Turrini et al. (2014). However, the analysis of well data drilled in the Ferrara salient (e.g., Bencini et al., 2011 ; ERS, 2009), coupled with the interpretation of seismic reflection data, documents the stratigraphic position and the properties of the shallower décollement. In particular, the analysis of caliper log in the San Felice sul Panaro 1 well (see supporting information, Figure S2) has shown a narrowing of the borehole in the late

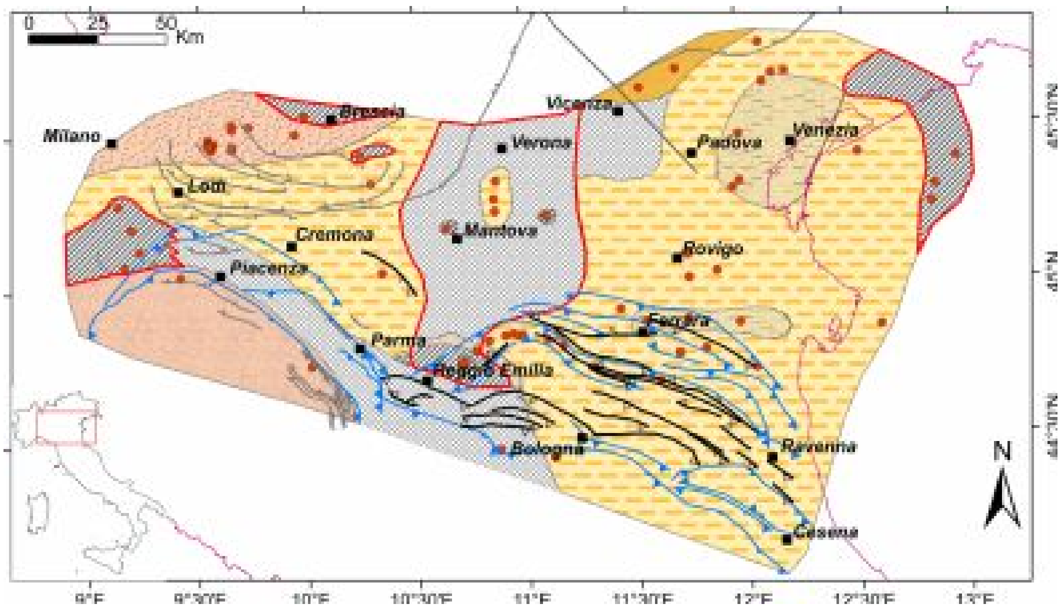

Figure 15. Map of the areal distribution of the late Eocene-lower Miocene formations, corresponding to the shallower décollement level, based on the analysis of well information and literature data (e.g., Dondi, Mostardini, & Rizzini, 1982 ; Dondi & D'Andrea, 1986). The following items are represented: areal distribution of the Cervarola Sandstones (1); Gallare Marls-Glauconie di Cavanella Fm. (2); Castelgomberto Calcarenites eq. (3); Gallare Marls (4); Gonfolite Fm.-Gallare Marls (5) and Castelgomberto Calcarenites (6); undefined formation areas (7); erosional/non depositional areas (8); elevated areas deduced from bibliographic data with reduced or absent sedimentation (9); location of wells that have drilled the late Eocene-Miocene formations (10); thrusts rooted in Oligocene shallow décollement (11); thrusts rooted in Upper Carnian deep décollement (12); other thrusts (13).

Eocene-lower Oligocene (2,312- to 2,319-m measured depth). This phenomenon has been attributed to the high plasticity of this horizon. Moreover, the analysis of the densities and the absorptions of the drilling muds in several wells (e.g., Bignardi 1, Bignardi 1 dir, and San Felice sul Panaro 1 wells) has also revealed an overpressured zone located within the late Eocene-Oligocene succession, with maximum overpressure values in correspondence with the aforementioned plastic interval (Bencini et al., 2011; ERS, 2009). The presence of this overpressured layer has been detected and documented in an area tens of kilometers wide. Therefore, the lithological characteristics and the presence of the overpressured interval make the late Eocene-Oligocene stratigraphic interval of the Gallare Marls an ideal candidate for tectonic décollement.

The map shown in Figure 15 highlights the control exerted by the presence/absence of the late Eocene Oligocene décollement on the areal distribution of the thrusts rooted in this shallow décollement. We reconstructed the distribution of the late Eocene-Oligocene (and Lower Miocene) formation based on the direct analysis of well stratigraphies integrated with a review of literature data (e.g., Dondi et al., 1982; Dondi & D'Andrea, 1986). For the late Eocene-Oligocene formations, the documented erosional-nondepositional areas are located South of Milan (e.g., Lacchiarella 1, Rea 1 dir, S. Genesio 1, and Valle Salimbene 1 wells), North and South of Brescia (e.g., Franciacorta 1 dir and Borgosatollo 1 wells), in the Bagnolo area north of Reggio Emilia (e.g., Bagnolo in piano, 1, 2, and 3 wells), between Mantova and Verona cities (e.g., Rodigo 1 and Bovolone 1 wells), and in the northern Adriatic area (e.g., Amanda 1 bis, Amira 1, and Rachele 1 wells). It should be noted that the morphological high represented by the Trento Plateau probably influenced the depositional processes during the late Eocene-Oligocene (e.g., Gallare Marls).

5. Discussion

5.1. Tectonic Style

There is a general consensus about the control exerted by some major décollement levels detected within the sedimentary cover of the Adriatic plate on the structural setting of the Northern Apennines thrust

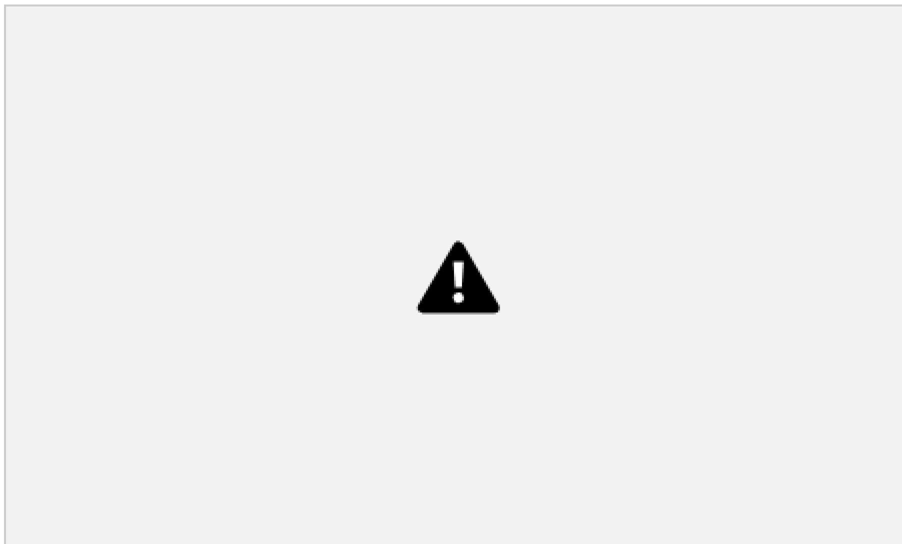

Figure 16. 3-D view of the basal décollement in the Upper Triassic (isobaths contour lines every 1,000 m). The green arrow indicates the north. The geological sections across the Cremona (C-C^0) and Ferrara (D-D^0) salients (Figure 11) are also shown together with seismicity during the period 1 January 2010 to 29 May 2012 (after ISIDE Working Group, 2015). The focal solution (after Govoni et al., 2014) and hypocenter of the 20 May mainshock (M_L 5.9) of the Emilia 2012 seismic sequence are projected on the section plane across the Ferrara salient (about 5 km from the west). Colored points correspond to hypocenter: large red points $M_L \geq 5$, medium orange points $4 \leq M_L \leq 4.9$, and small yellow points $3 \leq M_L \leq 3.9$.

system buried below the Po Plain (Carminati, Cavazza, et al., 2010; Maesano et al., 2015; Massoli et al., 2006; Ravaglia et al., 2006; Toscani et al., 2014, 2006). The two major décollements are generally recognized within the Cenozoic terrigenous sequence and at the base of the Mesozoic carbonates, although other minor décollement levels may also be identified (e.g., Fantoni et al., 2004).

A more complex and heterogeneous picture, with some differences in structural style between the Cremona and Ferrara salients and also within the Ferrara salient itself, has been recently pointed out by Turrini et al. (2014, 2016). In the western side of the Ferrara salient, Turrini et al. (2014, 2016) envisage two main décollements located along the top of the Triassic and the top of the crystalline basement while, in its eastern side, the top Triassic décollement is lacking with the basement likely involved by thrusting. In the same structural analysis, the Cremona salient is essentially due to thrusts and folds in the Cenozoic succession with the underlying carbonate substratum slightly displaced northward along a décollement likely located at the top of the crystalline basement. An involvement of basement slices in the external buried portion of the Northern Apennines thrust belt has also been proposed in several previous studies (e.g., Argnani et al., 2003; Artoni et al., 2010, 2007; Boccaletti et al., 2004; Capozzi & Picotti, 2009; Carannante et al., 2015; Fantoni et al., 2004; Fantoni & Franciosi, 2009, 2010; Lavecchia et al., 2012; Picotti et al., 2007; Picotti & Pazzaglia, 2008) that, in some cases, occurred through a reactivation of preexisting extensional faults (e.g., Carannante et al., 2015; Turrini et al., 2016).

In our integrated interpretation of well and seismic data (Figure 11) along the Cremona and Ferrara salients we have found clear evidences of two main décollement levels that, as discussed in detail in the previous sections, are located in the Upper Carnian and in the late Eocene-Oligocene formations, as already proposed in several other studies (e.g., Carminati, Cavazza, et al., 2010; Maesano et al., 2015; Massoli et al., 2006; Toscani et al., 2006). Published cross sections (among many others, Boccaletti et al., 2004; Cassano et al., 1986; Castellarin et al., 1985; Fantoni & Franciosi, 2010; Picotti et al., 2007; Pieri & Groppi, 1981) show that the basal décollement dips SW toward the hinterland of the accretionary prism, following the regional monocline. The 3-D view of the basal décollement (Figure 16) illustrates that, as also shown in our cross section (Figure 11), the dip of the basal detachment varies, moving from the Cremona to the Ferrara salient, from about 10° up to more than 20°.

The presence of inherited extensional faults has also been ascertained (e.g., Fantoni & Franciosi, 2010; Rogledi, 2010; Turrini et al., 2016), as shown in our cross sections (Figure 11). Some of these inherited extensional faults may have also influenced the enucleation of thrust ramps, also partly reactivated, as proposed,

Journal of Geophysical Research: Solid Earth 10.1002/2017JB015235

for instance, for the Mirandola structure by Bonini et al. (2014). Conversely, in our review of the available data set, we have not found any conclusive proof or evidence of basement involvement in the two analyzed salients.

Some of the differences in structural style discussed above are likely caused by the characteristics and quality of the seismic data available to the different researchers during their studies. As a matter of fact, although seismic interpretation is to a certain level a subjective process, the quality of the seismic data made available by the ViDEPI Project generally allows a fairly reliable interpretation down to the upper part of the Mesozoic carbonate substratum. The main differences among published interpretations arise in the deeper portion, near the base of the Upper Triassic formation and down to the basement, which is actually poorly resolved by the seismic data. A representative example of this consideration is provided by our cross section D-D^0 (Figure 11), which is built upon the interpretation of a regional seismic profile that has been already used to derive three other geological sections (i.e., Bonini et al., 2014; Carminati, Cavazza, et al., 2010; Lavecchia et al., 2012). A comparison of these published cross sections, also discussed by Bonini et al. (2016), highlights the quite good agreement between the structural settings described in the shallower part of the cross sections. On the contrary, the main thrusts deforming the Mirandola and the Ferrara trends are rooted in the basement in Lavecchia et al. (2012), although they merge into the Upper Carnian décollement in our cross section D-D^0 (Figure 11), as already proposed by Carminati, Cavazza, et al. (2010) and Bonini et al. (2014). Another example is provided by our cross section C-C^0 (Figure 11), which is very close to the cross section published by Picotti et al. (2007, Figure 5). In this case the Piadena structure is interpreted as an inverted preexisting extensional fault by Picotti et al. (2007), whereas the good quality profile we have had the opportunity to interpret (see Figure 5) shows that this structure is essentially due to the propagation of a ramp from the shallower décollement, as also proposed by Maesano and D'Ambrogi (2016).

The investigated area is seismically active, as also demonstrated by the Emilia earthquakes that occurred in May 2012 (Figures 1 and 16), with shortening rate obtained from Global Positioning System velocities in the order of 2–3 mm/year (Cuffaro et al., 2010; Michetti et al., 2012; Riguzzi et al., 2012; Vannoli et al., 2015). Seismic reflection profiles show active thrust tips at depth, even if fault planes are not reaching the surface. Pleistocene sediments are regularly tilted along the limbs of the frontal anticlines (e.g., Ferrara and Mirandola). The apparent low deformation of the frontal limbs of the external anticlines of the Apennines accretionary prism beneath the Po Basin may be a misleading signal due to strain partitioning during the coseismic stage in the context of high sedimentation rates (Daëron et al., 2007). As expected in typical fault-propagation folds, the 50–100 cm coseismic rupture at depth of 2–3 to 10 km (e.g., Tizzani et al., 2013) is transferred upward to slight folding, consistent with the tilt of the Upper Pleistocene sediments draping the frontal anticlines of the accretionary prism (e.g., between Tabiano 1 and S. Alessandro 1 wells in section C-C^0 in Figure 11).

Following the May 2012 Emilia earthquake, the analysis of the new seismological data, modeling of surface deformations, and seismotectonic interpretation of the existing subsurface data set have indisputably documented the activation of seismogenic thrusts within the Meso-Cenozoic sedimentary covers while leaving open the scientific debate regarding a possible activation of faults involving the basement (among many other, Argnani et al., 2016; Bonini et al., 2014; Bonini et al., 2016; Carannante et al., 2015; Govoni et al., 2014; Lavecchia et al., 2012; Tizzani et al., 2013; Turrini et al., 2015, 2016, and references therein).

Given the general agreement regarding the presence of the two regional décollements, which is well documented by the existing data set, and the inconclusive evidence of the presence of thrusts involving the basement, we believe that the thin-skinned reconstruction of the Cremona and Ferrara salients supported by high-quality seismic data (e.g., Figure 5) represents a conservative interpretation of the tectonic setting along this external segment of the Northern Apennines accretionary prism.

5.2. Factors Controlling Salient and Recess Development

In this study, we have better defined the characteristics of the two regional décollement levels. The vertical resolution provided by well data and depth-converted seismic reflection profiles (e.g., Figures 5 and 11) has allowed us to reliably constrain the stratigraphic position of the shallower décollement to the late Eocene Oligocene and that of the basal décollement to the Upper Carnian. Well data demonstrate that the shallower late Eocene-Oligocene décollement corresponds to overpressured shaly formations (i.e., Gallare Marls). Even

though the basal décollement has not been directly penetrated by boreholes within the thrust wedge, wells located very close to the thrust front provide evidence that the Upper Carnian basal décollement can be associated with mainly shaly units (i.e., San Giovanni Bianco Shales and Raibl Group).

Since the spatial coverage and resolution of the available data are limited, in order to tentatively map the areal distribution of the stratigraphic units hosting and controlling the location and depth of the décollement levels (which may disappear in some areas due to erosion or nondeposition), we have inte grated the analysis of well data and seismic reflection profiles with other published geological and geophy sical information (e.g., Bencini et al., 2011; Cassano et al., 1986; Dondi et al., 1982; Dondi & D'Andrea, 1986; ERS, 2009; Franciosi & Vignolo, 2002; Grandić et al., 2002; Ravaglia et al., 2006). In particular, since a direct well control for the Triassic units is missing within the thrust structures associated with the Cremona and Ferrara salients, the Upper Carnian map is affected by unavoidable uncertainties. However, notwithstanding these uncertainties, the evident match between the erosional-nondepositional areas, derived by completely independent geophysical data, and the geometry of the salient-recess system should be noted. Although the lateral variations of the stratigraphic units hosting the décollement are controlled by the inher ited architecture of the Mesozoic Tethyan passive continental margin, the comparison between the distribu tion of recognized thrusts and the Mesozoic paleogeography highlights that the geometry of the Northern Apennines system of salients-recesses does not directly correspond with a simple relationship to the transi tions between the Trento Plateau and the Lombard and North Adriatic basins (Figure 9). As an example, the presence of the supposedly low friction Upper Carnian basal décollement within the more rigid Triassic carbonates of the Trento Plateau (Figure 13) has prevented this paleogeographic domain from behaving as a rigid obstacle with respect to the propagation of the orogenic front, allowing the upper block to detach from the lower one. For this reason, the eastern part of the horst was involved in the structuring of the western part of the Ferrara salient (Figure 9). However, the presence of the Trento Plateau influenced the depositional processes responsible for the development of the late Eocene-Oligocene formations (Gallare Marls) that localize the propagation of the shallow décollement (Figure 15).

The map with the first activation age for the Northern Apennines thrusts (Figure 12) reveals that along the Ferrara salient thrust faults propagated toward the foreland in Neogene times while along the Cremona salient thrust fault remained essentially stationary since Messinian time. Our results point out that among the different factors influenced by the architecture of the predeformational sedimentary basin (e.g., depth to décollement, rock strength, décollement strength, and décollement slope), two parameters have played a primary role in shaping the arcs of the Northern Apennines thrust front: (i) the areal distribution and the lateral facies variations of the shaly units hosting the décollement levels and (ii) the slope of the basal décollement. Accordingly, following the definitions proposed by Marshak (2004), the genesis of the Northern Apennines arcs can be considered, in a broad sense, "décollement-controlled." The combined influ ence of across-strike changes in the décollement properties and the basement curvature has been already analyzed in previous researches (e.g., the external central Betics; Jimenez-Bonilla et al., 2016). Although a quantitative mechanical modeling to test the implications of changing sediment thickness above the main basal décollement and to evaluate lateral changes in the mechanical behavior of the décollement has not been carried out, the Northern Apennines case study illustrates the influence of along-strike variation of these two relevant parameters. Specifically, this example suggests that the development of a salient-recess system mainly controlled by the areal distribution of the décollement levels may be enhanced by along-strike changes in the slope of the basal décollement induced by anisotropies in the flexural behavior of the subducting slab.

It is well known that the mechanical properties of the basal décollement exert a relevant control in determin ing how a thrust belt deforms, as documented in the Salt Ranges of Northern Pakistan, Jura Mountains, or Franklin Mountains in northwestern Canada (among many others, Butler et al., 1987; Calassou et al., 1993; Cotton & Koyi, 2000; Davis & Engelder, 1985). Ductile and frictional décollements have been defined as the two possible end-members, which produce different styles of deformation (Bahroudi & Koyi, 2003; Li & Mitra, 2017). As an example, the presence of a weak salt décollement allows the thrust belt to have a narrow cross-sectional taper associated with a thrust front propagating quickly toward the foreland and with syn chronous development of thrust structures (Cotton & Koyi, 2000; Davis & Engelder, 1985; Ford, 2004). However, according to our review, well data do not support the presence of any significant salt layer in

correspondence to the Northern Apennines basal décollement. Moreover, the absence of any diapiric struc ture is not in agreement with the presence of a low friction salt décollement.

While the anisotropies on thrust belts evolution caused by lateral transitions from a low friction to an high friction basal décollement have been documented by both analogue and numerical models (e.g., Calassou et al., 1993; Li & Mitra, 2017; Macedo & Marshak, 1999; Ruh, Gerya, & Burg, 2013, 2017), the Northern Apennines provides evidences of how the development of a salient-recess system may be determined by along-strike variation of mainly shaly décollement levels. In this case study, as already suggested by Castellarin et al. (1985), the erosional-nondepositional areas of the Upper Carnian and of the late Eocene Oligocene regional shaly décollements have prevented the propagation of thrust faults, favoring the conse quent formation of recesses, while depositional areas have allowed thrust advancement toward the foreland and the consequent formation of salients.

Thrust belts and accretionary prisms have a wedge-shaped configuration in cross section (Dahlen, 1990; Dahlen, Suppe, & Davis, 1984; Davis et al., 1983) defined by the upper slope of the wedge, usually rising toward the hinterland (angle α), and by the basal décollement that, dipping toward the hinterland, is nearly parallel to the foreland monocline (angle β). The relevance of the angle β has been discussed in several works (Bigi et al., 2003; Boyer, 1995; Doglioni, 1994; Ford, 2004; Koyi & Vendeville, 2003; Lenci & Doglioni, 2007; Mariotti & Doglioni, 2000; Mitra, 1997). It is well known that according to the principles of the critical taper model (Dahlen, 1990; Dahlen, Suppe, & Davis, 1984; Davis et al., 1983), a steeper basal décollement (i.e., a higher angle β) induces a wider thrust belt associated with a minor internal shortening and a faster rate of frontal thrust propagation (Marshak, 2004) as also documented in the Wyoming and Provo salients of the Sevier thrust belt in Utah (Boyer, 1995; Mitra, 1997). A steeper foreland monocline, controlled by the flexure of the lower plate, also produces an increasing depth to décollement and a thicker sedimentary cover both in the foredeep and in the depositional wedge top (Lenci et al., 2004; Mariotti & Doglioni, 2000). It has been also suggested (Perrin et al., 2016) that the length and width of the thrust zone splaying off the principal décollement might scale to the length of the décollement itself representing a possible further factor control ling the variability in the across-strike extent of a salient.

Since the top of the Northern Apennine wedge mainly acted as a depositional surface during the thrust belt evolution, the angle α remained at value of about zero or even negative (Doglioni, 1993; Doglioni & Prosser, 1997). Consequently, the taper angle is essentially controlled by the angle β. The variation of the angle β along the Northern Apennines arcs has been analyzed in several papers (Bigi et al., 2003; Ford, 2004; Lenci & Doglioni, 2007; Mariotti & Doglioni, 2000). As also evident in our cross sections (Figures 11 and 16), the basal décollement and the foreland monocline show a steeper geometry in the Ferrara salient (up to more than 20°) than in the Cremona salient (up to about 10°).

These β angles were gradually attained since upper Miocene times following the progressive flexure of the westward subducting and eastward retreating Adriatic lithosphere (e.g., Carminati, Doglioni, & Scrocca, 2003; Doglioni, 1991; Faccenna et al., 2003; Ford, 2004; Malinverno & Ryan, 1986; Patacca et al., 1992; Rosenbaum & Lister, 2004; Royden et al., 1987; Scrocca et al., 2007; Turrini et al., 2014, 2016). Assuming that the properties of the Upper Carnian geological formations remain almost the same, the steeper basal décollement in the Ferrara salient could explain the more pronounced propagation of the thrust front in this area.

6. Conclusions

The Northern Apennines accretionary prism front is buried below a thick succession of Plio-Quaternary fore deep deposits and is characterized by an undulating geometry. In the study area, the thrust front is charac terized by two more advanced sectors, the Cremona and Ferrara salients, separated by a less advanced zone, the Parma recess (Figures 1 and 12).

The analysis of the available data shows that in the study area, below the active margin deposits, the predo minantly Mesozoic passive margin succession consists of horsts and grabens. These paleographic domains, from west to east, are as follows: (i) the Lombard Basin, (ii) the Trento Plateau, and (iii) the North Adriatic Basin (Figures 6–10).

The reinterpretation of a mainly preexisting data set documents the thin-skinned tectonic style of the Northern Apennines thrust system buried beneath the Po Basin, which is controlled by two main regional

and late Eocene-Oligocene décollement levels (Figures 13 and 15, respectively) have been defined based on well data analysis and published information (e.g., Cassano et al., 1986; Dondi et al., 1982; Dondi & D'Andrea, 1986; Grandić et al., 2002). For both levels, erosional-nondepositional areas have been also identified.

The comparison between the structural and stratigraphic frameworks of the study area reveals the following:

1. There is an offset between the location and the extent of the Parma recess and the Trento Plateau; the two trends are oblique to each other (Figure 9).
2. There is a poor correspondence between the apexes of the arcs and the depocenters of the Mesozoic basins (Figure 9).
3. There is a good correlation between the position of the Parma recess and the location and extent of the erosional-nondepositional areas of the formations associated with the basal (Upper Carnian; Figure 13) and shallow (late Eocene-Oligocene; Figure 15) décollements.

These observations indicate that Northern Apennines arcs can be defined as basin-controlled (in the sense of, Macedo & Marshak, 1999). The origin of the salients and of the intervening recess is primarily controlled by lateral facies variations of the stratigraphic units hosting the décollement levels, which may disappear in some areas due to Meso-Cenozoic erosion or nondeposition.

Moreover, the analysis of the basal décollement isobath map shows a larger forward propagation of the thrust system over steeper segments of the basal décollement (Figure 16), in agreement with the known mechanics of thrust belts. Since the basal décollement is nearly parallel to the foreland monocline, it can be concluded that the flexural behavior of the Adriatic subducting slab significantly contributed to the final shape of the Northern Apennines arcs.

Acknowledgments

décollement levels (Figures 8 and 11). A basal décollement level developed in the Upper Carnian units (i.e., San Giovanni Bianco Clay and Raibl Group, around 227–237 Ma), whereas a shallower décollement level is located in the late Eocene-Oligocene formations (i.e., Gallare Marls, around 23–37 Ma). Known lithological and petrophysical properties confirm that these formations can act as décollement levels.

The areal extension and facies variation of the stratigraphic units hosting and controlling the location and depth of the Upper Carnian

References

GasPlus Italiana S.r.l. company is grate fully acknowledged for the collabora tion and for making available the seismic reflection profile shown in Figure 5 of this paper. The other data used in this work are from the website of the ViDEPI Project (Visibility of petro leum exploration data in Italy, Ministry of Economic Development, National Mining Office for Hydrocarbons and Earth Resources, http://unmig.svilup poeconomico.gov.it/videpi/videpi.asp) and from cited references. Midland Valley is acknowledged for providing Move software, which has been utilized to produce the two geological cross sections. This paper benefited from fruitful discussions with Roberto Bencini. The Associate Editor, two anonymous reviewer, Giancarlo Molli, Olivier Lacombe, and Jacques
Malavieille provided constructive criti cisms that greatly improved the quality of our manuscript.

Aitken, J. D., & Long, D. G. F. (1978). Mackenzie tectonic arc-reflection of early basin configuration? *Geology*, *6*(10), 626–629. https://doi.org/10.1130/0091-7613(1978)6%3C626:MTAOEB%3E2.0.CO;2
Albano, M., Barba, S., Tarabusi, G., Saroli, M., & Stramondo, S. (2017). Discriminating between natural and anthropogenic earthquakes: Insights from the Emilia Romagna (Italy) 2012 seismic sequence. *Scientific Reports*, *282*, 7.
Allen, M. B., & Talebian, M. (2011). Structural variation along the Zagros and the

nature of the Dezful Embayment. *Geological Magazine*, *148*(5–6), 911–924. https://doi.org/10.1017/S0016756811000318
Argand, E. (1916). Sur l'arc des Alpes occidentales. *Eclogae Geologicae Helvetiae*, *14*, 145–191.
Argand, E. (1924). La tectonique de l'Asie. In *Proceedings of the 13th International Geology Congress* (Vol. 7, pp. 171–372). Argnani, A., Barbacini, G., Bernini, M., Camurri, F., Ghielmi, M., Papani, G., et al. (2003). Gravity tectonics driven by Quaternary uplift in the Northern Apennines: Insights from the La Spezia-Reggio Emilia geo-transect. *Quaternary International*, *101*, 13–26. Argnani, A., Carannante, S., Massa, M., Lovati, S., & D'Alema, E. (2016). Reply to the "Comment on "The May 1 20 (MW 6.1) and 29 (MW 6.0), 2012, Emilia (Po Plain, northern Italy) earthquakes: New seismotectonic implications from subsurface geology and high-quality hypo center location" by Carannante et al., 2015" by Bonini L., et al. *Tectonophysics*, *693*, 157–162.
Artoni, A., Bernini, M., Papani, G., Rizzini, F., Barbacini, G., Rossi, M., et al. (2010). Mass-transport deposits in confined wedge-top basins: Surficial processes shaping the Messinian orogenic wedge of Northern Apennine of Italy. *Italian Journal of Geosciences*, *129*(1), 101–118. https://doi.org/10.3301/IJG.2009.09
Artoni, A., Rizzini, F., Roveri, M., Gennari, R., Manzi, V., Papani, G., & Bernini, M. (2007). Tectonic and climatic controls on sedimentation in Late Miocene Cortemaggiore Wedge-Top Basin (Northwestern Apennines, Italy). In O. Lacombe, et al. (Eds.), *Thrust Belts and Foreland Basin* (pp. 431–456). Berlin: Springer. https://doi.org/10.1007/978-3-540-69426-7_23
Bahroudi, A., & Koyi, H. A. (2003). Effect of spatial distribution of Hormuz salt on deformation style in the Zagros fold and thrust belt: An analogue modelling approach. *Journal of the Geological Society*, *160*(5), 719–733. https://doi.org/10.1144/0016-764902-135 Bencini, R., Alimonti, C., Bianchi, E., Borgatti, L., Carminati, E., De Mattia, R., et al. (2011). Metodologia di valutazione dell'idoneità di un sito di stoccaggio sotterraneo di gas naturale. V Congresso Nazionale dell'Associazione Italiana Gestione Energia (AIGE), Modena, 8–9 June 2011.
Benedetti, L. C., Tapponnier, P., Gaudemer, Y., Manighetti, I., & van der Woerd, J. (2003). Geomorphic evidence for an emergent active thrust along the edge of the Po Plain: The Broni-Stradella fault. *Journal of Geophysical Research*, *108*(B5), 2238. https://doi.org/10.1029/ 2001JB001546
Bennett, R. A., Serpelloni, E., Hreinsdóttir, S., Brandon, M. T., Buble, G., Basic, T., et al. (2012). Syn-convergent extension observed using the RETREAT GPS network, northern Apennines, Italy. *Journal of Geophysical Research*, *117*, B04408. https://doi.org/10.1029/2011JB008744 Bernini, M., & Papani, G. (1987). Alcune considerazioni sulla struttura del margine appenninico emiliano fra il T. Stirone ed il T. Enza (e sue relazioni con il Sistema del Taro), Conference proceedings, Brittle deformation analysis in neotectonics, Firenze, 17 April 1986, L'Ateneo Parmense.

Bertello, F., Fantoni, R., Franciosi, R., Gatti, V., Ghielmi, M., & Pugliese, A. (2010). From thrust-and-fold belt to foreland: Hydrocarbon occur rences in Italy. In B. A. Vining & S. C. Pickering (Eds.), *Petroleum Geology: From Mature Basin to New Frontiers*, *Proceedings of the 7th pet roleum geology conference* (pp. 112–113). London: Geological Society. https://doi.org/10.1144/0070113
Bertotti, G., Picotti, V., Bernoulli, D., & Castellarin, A. (1993). From rifting to drifting: Tectonic evolution of the south-Alpine upper crust from the Triassic to the Early Cretaceous. *Sedimentary Geology*, *86*(1-2), 53–76. https://doi.org/10.1016/0037-0738(93)90133-P
Bertotti, G., Picotti, V., & Cloetingh, S. (1998). Lithospheric weakening during "retro-foreland" basin formation: Tectonic evolution of the central South Alpine foredeep. *Tectonics*, *17*, 131–142. https://doi.org/10.1029/97TC02066
Bigi, S., Lenci, F., Doglioni, C., Moore, J. C., Carminati, E., & Scrocca, D. (2003). Décollement depth versus accretionary prism dimension in the Apennines and the Barbados. *Tectonics*, *22*(2), 1010. https://doi.org/10.1029/2002TC001410
Boccaletti, M., Bonini, M., Corti, G., Gasperini, P., Martelli, L., Piccardi, L., et al. (2004). *Seismotectonic map of the Emilia-Romagna Region* (Scale 1:250,000). SELCA, Firenze, Italy: Regione Emilia-Romagna-CNR.
Boccaletti, M., Corti, G., & Martelli, L. (2011). Recent and active tectonics of the external zone of the Northern Apennines (Italy). *International Journal of Earth Sciences*, *100*(6), 1331–1348. https://doi.org/10.1007/s00531-010-0545-y
Bonini, L., Toscani, G., & Seno, S. (2014). Three-dimensional segmentation and different rupture behavior during the 2012 Emilia seismic sequence (Northern Italy). *Tectonophysics*, *630*, 33–42. https://doi.org/10.1016/j.tecto.2014.05.006
Bonini, L., Toscani, G., & Seno, S. (2016). Comment on "The May 20 (M W 6.1) and 29 (M W 6.0), 2012, Emilia (Po Plain, Northern Italy) earthquakes: New seismotectonic implications from subsurface geology and high-quality hypocenter location" by Carannante et al., 2015. *Tectonophysics*, *688*, 182–188. https://doi.org/10.1016/j.tecto.2016.02.001
Boyer, S. E. (1995). Sedimentary basin taper as a factor controlling the geometry and advance of thrust belts. *American Journal of Science*, *295*(10), 1220–1254. https://doi.org/10.2475/ajs.295.10.1220
Butler, R. W., Coward, M. P., Harwood, G. M., & Knipe, R. J. (1987). Salt control on thrust geometry, structural style and gravitational collapse along the Hymalayan Mountain Front in the Salt Ranges of Northern Pakistan. In I. Lerche & J. J. O'Brien (Eds.), *Dynamic Geology of Salt and Related Structures* (pp. 399–417). Academic Press: London. https://doi.org/10.1016/B978-0-12-444170-5.50013-0
Calassou, S., Larroque, C., & Malavieille, J. (1993). Transfer zones of deformation in thrust wedges: An experimental study. *Tectonophysics*, *221*(3-4), 325–344. https://doi.org/10.1016/0040-1951(93)90165-G
Capozzi, R., & Picotti, V. (2009). The residual potential of the northern Apennine petroleum system a geochemical and structural study of spontaneous seeps. AAPG European Regional Annual Conference, Paris-Malmaison, France, 23–24 November 2009.
Carannante, S., Argnani, A., Massa, M., D'Alema, E., Lovati, S., Moretti, M., et al. (2015). The May 20 (MW 6.1) and 29 (MW 6.0), 2012, Emilia (Po plain, Northern Italy) earthquakes: New seismotectonic implications from subsurface geology and high-quality hypocenter location. *Tectonophysics*, *655*, 107–123. https://doi.org/10.1016/j.tecto.2015.05.015
Carey, S. W. (1955). The orocline concept in geotectonics, part I. *Papers and Proceedings of the Royal Society of Tasmania*, *89*, 255–288.
Carminati, E., Cavazza, D., Scrocca, D., Fantoni, R., Scotti, P., & Doglioni, C. (2010). Thermal and tectonic evolution of the Southern Alps (Northern Italy) rifting: Coupled organic matter maturity analysis and thermo-kinematic modelling. *American Association of Petroleum Geologists Bulletin*, *94*(3), 369–397. https://doi.org/10.1306/08240909069
Carminati, E., Doglioni, C., & Scrocca, D. (2003). Apennines subduction-related subsidence of Venice (Italy). *Geophysical Research Letters*, *30*(13), 1717. https://doi.org/10.1029/2003GL017001
Carminati, E., Doglioni, C., & Scrocca, D. (2004). Alps vs. Apennines. *Special Volume of the Italian Geological Society for the 32° International Geological Congress* (pp 141–151).
Carminati, E., & Martinelli, G. (2002). Subsidence rates in the Po Plain, northern Italy: The relative impact of natural and anthropogenic causation. *Engineering Geology*, *66*(3-4), 241–255. https://doi.org/10.1016/S0013-7952(02)00031-5
Carminati, E., Scrocca, D., & Doglioni, C. (2010). Compaction-induced stress variations with depth in an active anticline: Northern Apennines, Italy. *Journal of Geophysical Research*, *115*, B02401. https://doi.org/10.1029/2009JB006395
Casero, P., Rigamonti, A., & Iocca, M. (1990). Paleogeographic relationships during Cretaceous between the Northern Adriatic area and the Eastern Southern Alps. *Memorie della Societa Geologica Italiana*, *45*, 807–814.
Cassano, E., Anelli, A., Fichera, R., & Cappelli, V. (1986). Pianura Padana: interpretazione integrata di dati geologici e geofisici. Proceedings of the 73th Meeting of the Società Geologica Italiana, Rome (Italy), 29 September-4 October.
Castellarin, A., Eva, C., Ciglia, G., & Vai, G. B. (1985). Analisi strutturale del Fronte Appenninico Padano. *Giornale di Geologia*, *47*(1,2), 47–75.
Cati, A., Sartorio, D., & Venturini, S. (1987). Carbonate platforms in the subsurface of the northern Adriatic Sea. *Memorie della Societa Geologica Italiana*, *40*, 295–308.
Consiglio Nazionale delle Ricerche (1992). Structural Model of Italy and Gravity Map, Progetto Finalizzato Geodinamica. Quaderni de "La Ricerca Scientifica," 114, Vol. 3.

Costa, M. (2003). The buried, Apenninic arcs of the Po Plain and northern Adriatic Sea (Italy): A new model. *Bollettino della Societa Geologica Italiana*, *122*, 3–23.
Cotton, J. T., & Koyi, H. A. (2000). Modeling of thrust fronts above ductile and frictional detachments: Application to structures in the Salt Range and Potwar Plateau, Pakistan. *Geological Society of America Bulletin*, *112*(3), 351–363. https://doi.org/10.1130/0016-7606(2000)112%3C351:MOTFAD%3E2.0.CO;2
Cuffaro, M., Riguzzi, F., Scrocca, D., Antonioli, F., Carminati, E., Livani, M., & Doglioni, C. (2010). On the geodynamics of the northern Adriatic plate. *Rendiconti Fisici dell'Accademia dei Lincei*, *21*(S1), 253–279. https://doi.org/10.1007/s12210-010-0098-9
Daëron, M., Avouac, J. P., & Charreau, J. (2007). Modeling the shortening history of a fault tip fold using structural and geomorphic records of deformation. *Journal of Geophysical Research*, *112*, B03S13. https://doi.org/10.1029/2006JB004460
Dahlen, F. A. (1990). Critical taper model of fold and thrust belts and accretionary wedges. *Annula Review of Earth and Planetary Sciences*, *18*(1), 55–99. https://doi.org/10.1146/annurev.ea.18.050190.000415
Dahlen, F. A., Suppe, J., & Davis, D. (1984). Mechanics of foldand-thrust belts and accretionary wedges: Cohesive coulomb theory. *Journal of Geophysical Research*, *89*, 10,087–10,101. https://doi.org/10.1029/JB089iB12p10087
Dana, J. D. (1866). Observations on the origin of some of the Earth's features. *American Journal of Science*, *42*(125), 205–253.
Davis, D., Suppe, J., & Dahlen, F. A. (1983). Mechanics of fold-and-thrust belts and accretionary wedges. *Journal of Geophysical Research*, *88*, 1153–1172. https://doi.org/10.1029/JB088iB02p01153
Davis, D. M., & Engelder, T. (1985). The role of salt in fold-and-thrust belts. *Tectonophysics*, *119*(1-4), 67–88. https://doi.org/10.1016/0040-1951(85)90033-2
Davis, D. M., & Lillie, R. J. (1994). Changing mechanical response during continental collision: Active examples from the foreland thrust belts of Pakistan. *Journal of Structural Geology*, *16*(1), 21–34. https://doi.org/10.1016/0191-8141(94)90015-9

Devoti, C., Riguzzi, F., Cuffaro, M., & Doglioni, C. (2008). New GPS constraints on the kinematics of the Apennines subduction. *Earth and Planetary Science Letters*, *273*(1-2), 163–174. https://doi.org/10.1016/j.epsl.2008.06.031
DISS Working Group (2015). Database of Individual Seismogenic Sources (DISS), Version 3.2.0: A compilation of potential sources for earthquakes larger than M 5.5 in Italy and surrounding areas. http://diss.rm.ingv.it/diss/, Istituto Nazionale di Geofisica e Vulcanologia. https://doi.org/10.6092/INGV.IT-DISS3.2.0
Dixon, J. S. (1982). Regional structural synthesis, Wyoming salient of the western Overthrust Belt. *American Association of Petroleum Geologists Bulletin*, *10*, 1560–1580.
Doglioni, C. (1991). A proposal for the kinematic modelling of W-dipping subductions – Possible applications to the Tyrrhenian-Apennines system. *Terra Nova*, *3*(4), 423–434. https://doi.org/10.1111/j.1365-3121.1991.tb00172.x
Doglioni, C. (1993). Some remarks on the origin of foredeeps. *Tectonophysics*, *288*, 1–20.
Doglioni, C. (1994). Foredeeps versus subduction zones. *Geology*, *22*(3), 271–274. https://doi.org/10.1130/0091-7613(1994)022%3C0271:FVSZ%3E2.3.CO;2
Doglioni, C., Barba, S., Carminati, E., & Riguzzi, F. (2011). Role of the brittle-ductile transition on fault activation. *Physics of the Earth and Planetary Interiors*, *184*(3-4), 160–171. https://doi.org/10.1016/j.pepi.2010.11.005
Doglioni, C., Barba, S., Carminati, E., & Riguzzi, F. (2015). Fault on-off versus strain rate and earthquakes energy. *Geoscience Frontiers*, *6*(2), 265–276. https://doi.org/10.1016/j.gsf.2013.12.007
Doglioni, C., Gueguen, E., Harabaglia, P., & Mongelli, F. (1999). On the origin of west-directed subduction zones and applications to the western Mediterranean. In B. Durand, L. Jolivet, F. Horvath, & M. Seranne (Eds.), *The Mediterranean Basins: Tertiary Extension Within the Alpine Orogen*, *Geology Society of London, Special Publication, 156*, 541–561.
Doglioni, C., Harabaglia, P., Merlini, S., Mongelli, F., Peccerillo, A., & Piromallo, C. (1999). Orogens and slabs vs. their direction of subduction. *Earth-Science Reviews*, *45*(3-4), 167–208. https://doi.org/10.1016/S0012-8252(98)00045-2
Doglioni, C., & Prosser, G. (1997). Fold uplift versus regional subsidence and sedimentation rate. *Marine and Petroleum Geology*, *14*(2), 179–190. https://doi.org/10.1016/S0264-8172(96)00065-7
Dominguez, S., Lallemand, S. E., Malavieille, J., & von Huene, R. (1998). Upper plate deformation associated with seamount subduction. *Tectonophysics*, *293*(3-4), 207–224. https://doi.org/10.1016/S0040-1951(98)00086-9
Dominguez, S., Malavieille, J., & Lallemand, S. E. (2000). Deformation of accretionary wedges in response to seamount subduction: Insights from sandbox experiments. *Tectonics*, *19*, 182–196. https://doi.org/10.1029/1999TC900055
Dondi, L., & D'Andrea, M. G. (1986). La Pianura Padana e Veneta dall'Oligocene superiore al Pleistocene. *Giornale di Geologia*, *48*(1, 2), 197–225.
Dondi, L., Mostardini, F., & Rizzini, A. (1982). Evoluzione sedimentaria e paleogeografica nella Pianura Padana, in Guida alla geologia del margine appenninico padano. In G. Cremonini, & F. Ricci Lucchi (Eds.), *Guida alla Geologia del Margine Appenninico Padano* (pp. 47–58). Società Geologica Italiana: Bologna.
ERS (2009). *Studio multidisciplinare del sottosuolo dell'area di Rivara, Studio di impatto ambientale-Progetto Rivara* (p. 193). Rome, Italy: ERG Rivara Storage.
Faccenna, C., Jolivet, L., Piromallo, C., & Morelli, A. (2003). Subduction and the depth of convection in the Mediterranean mantle. *Journal of Geophysical Research*, *108*(B2), 2099. https://doi.org/10.1029/2001JB001690
Fantoni, R., Bersezio, R., & Forcella, F. (2004). Alpine structure and deformation chronology at the Southern Alps-Po plain border in Lombardy. *Bollettino della Societa Geologica Italiana*, *123*(3), 463–477.
Fantoni, R., & Franciosi, R. (2009). Mesozoic extension and Cenozoic compression in Po Plain and Adriatic foreland. *Rendiconti Online della Società Geologica Italiana*, *9*, 28–31.
Fantoni, R., & Franciosi, R. (2010). Tectono-sedimentary setting of the Po Plain and Adriatic Foreland. *Rendiconti Fisici dell'Accademia dei Lincei*, *21*(S1), 197–209. https://doi.org/10.1007/s12210-010-0102-4
Fantoni, R., & Scotti, P. (2003). Thermal record of the Mesozoic extensional tectonics in the Southern Alps. *Atti Ticinesi di Scienza della Terra*, *9*, 96–101.
Ferrill, D. A., & Groshong, R. H. (1993). Kinematic model for the curvature of the northern Subalpine Chain, France. *Journal of Structural Geology*, *15*(3-5), 523–541. https://doi.org/10.1016/0191-8141(93)90146-2
Ford, M. (2004). Depositional wedge tops: Interaction between low basal friction external orogenic wedges and flexural foreland basins. *Basin Research*, *16*(3), 361–375. https://doi.org/10.1111/j.1365-2117.2004.00236.x
Franciosi, R., & Vignolo, A. (2002). Northern Adriatic Foreland: a promising setting for the Southalpine Midtriassic petroleum system. Extended Abstracts Book (pp. 1–4) Florence: EAGE conference.
Galli, P., Castenetto, S., & Peronace, E. (2012). May 2012 Emilia earthquakes (mw 6, northern Italy): Macroseismic effects distribution and seismotectonic implications. *Alpine and Mediterranean Quaternary*, *25*(2), 105–123.

Ghielmi, M., Minervini, M., Nini, C., Rogledi, S., & Rossi, M. (2013). Late Miocene-middle Pleistocene sequences in the Po Plain-Northern Adriatic Sea (Italy): The stratigraphic record of modification phases affecting a complex foreland basin. *Marine and Petroleum Geology*, *42*, 50–81. https://doi.org/10.1016/j.marpetgeo.2012.11.007

Ghielmi, M., Minervini, M., Nini, C., Rogledi, S., Rossi, M., & Vignolo, A. (2010). Sedimentary and tectonic evolution in the eastern Po-Plain and northern Adriatic Sea area from Messinian to middle Pleistocene (Italy). *Rendiconti Fisici dell'Accademia dei Lincei*, *21*(S1), 131–166. https://doi.org/10.1007/s12210-010-0101-5

Govoni, A., Marchetti, A., De Gori, P., Di Bona, M., Lucente, F. P., Improta, L., et al. (2014). The 2012 Emilia seismic sequence (Northern Italy): Imaging the thrust fault system by accurate aftershock location. *Tectonophysics*, *622*(21), 44–55. https://doi.org/10.1016/j.tecto.2014.02.013

Grandić, S., Biancone, M., & Samarzˇija, J. (2002). Geophysical and stratigraphic evidence of the Adriatic Triassic rift structures. *Memorie della Societa Geologica Italiana*, *57*, 315–325.

Grenerczy, G., Sella, G., Stein, S., & Kenyeres, A. (2005). Tectonic implications of the GPS velocity field in the northern Adriatic region. *Geophysical Research Letters*, *32*, L16311. https://doi.org/10.1029/2005GL022947

Hindle, D., & Burkhard, M. (1999). Strain, displacement and rotation associated with the formation of curvature in fold belts; the example of the Jura arc. *Journal of Structural Geology*, *21*(8-9), 1089–1101. https://doi.org/10.1016/S0191-8141(99)00021-8

Homberg, C., Lacombe, O., Angelier, J., & Bergerat, F. (1999). New constraints for indentation mechanisms in arcuate belts from the Jura Mountains, France. *Geology*, *27*(9), 827–830. https://doi.org/10.1130/0091-7613(1999)027%3C0827:NCFIMI%3E2.3.CO;2

International Commission on Hydrocarbon Exploration and Seismicity in the Emilia region (2014). *Report on the hydrocarbon exploration and seismicity in Emilia region* (213 pp.). International Commission on Hydrocarbon Exploration and Seismicity in the Emilia region. Retrived from http://mappegis.regione.emilia-romagna.it/gstatico/documenti/ICHESE/ICHESE_Report.pdf

ISIDE Working Group. (2015). Italian seismological instrumental and parametric database. http://iside.rm.ingv.it

Jimenez-Bonilla, A., Torvela, T., Balanyá, J. C., Expósito, I., & Díaz-Azpiroz, M. (2016). Changes in dip and frictional properties of the basal detachment controlling orogenic wedge propagation and frontal collapse: The external central Betics case. *Tectonics*, *35*, 3028–3049. https://doi.org/10.1002/2016TC004196

Koyi, H. A., & Vendeville, B. C. (2003). The effect of décollement dip on geometry and kinematics of model accretionary wedges. *Journal of Structural Geology*, *25*(9), 1445–1450. https://doi.org/10.1016/S0191-8141(02)00202-X

Lacombe, O., Mouthereau, F., Angelier, J., Chu, H. T., & Lee, J. C. (2003). Frontal belt curvature and oblique ramp development at an obliquely collided irregular margin: Geometry and kinematics of the NW Taiwan fold-thrust belt. *Tectonics*, *22*(3), 1025. https://doi.org/10.1029/2002TC001436

Lake, P. (1931). Island arcs and mountain building. *Geographical Journal*, *78*(2), 149–160. https://doi.org/10.2307/1784446

Laubscher, H. P. (1972). Some overall aspects of Jura dynamics. *American Journal of Science*, *272*, 93–304.

Laubscher, H. P. (1985). Large-scale, thin-skinned thrusting in the southern Alps: Kinematic models. *Geological Society of America Bulletin*, *96*(6), 710–718. https://doi.org/10.1130/0016-7606(1985)96%3C710:LTTITS%3E2.0.CO;2

Lavecchia, G., De Nardis, R., Cirillo, D., Brozzetti, F., & Boncio, P. (2012). The May-June 2012 Ferrara Arc earthquakes (northern Italy): Structural control of the spatial evolution of the seismic sequence and of the surface pattern of coseismic fractures. *Annals of Geophysics*, *55*, 4. https://doi.org/10.4401/ag-6173

Lawton, T. F., Boyer, S. E., & Schmitt, J. G. (1994). Influence of inherited taper on structural variability and conglomerate distribution, Cordilleran fold and thrust belt, western United States. *Geology*, *22*(4), 339–342. https://doi.org/10.1130/0091-7613(1994)022%3C0339:IOITOS%3E2.3.CO;2

Lenci, F., Carminati, E., Doglioni, C., & Scrocca, D. (2004). Basal décollement and subduction depth vs. topography in the Apennines-Calabrian arc. *Bollettino della Societa Geologica Italiana*, *123*, 497–502.

Lenci, F., & Doglioni, C. (2007). On some geometric prism ssymmetries. In O. Lacombe, J. Lavé, F. Roure, & J. Verges (Eds.), *Thrust Belts and Foreland Basins: From Fold Kinematics to Hydrocarbon Systems*, *Frontiers in Earth Sciences* (pp. 41–60). Berlin: Springer. https://doi.org/10.1007/978-3-540-69426-7_2

Li, J., & Mitra, S. (2017). Geometry and evolution of fold-thrust structures at the boundaries between frictional and ductile detachments. *Marine and Petroleum Geology*, *85*, 16–34. https://doi.org/10.1016/j.marpetgeo.2017.04.011

Lickorish, W. H., Ford, M., Buergisser, J., & Cobbold, P. R. (2002). Arcuate thrust systems in sandbox experiments; A comparison to the external arcs of the Western Alps. *Geological Society of America Bulletin*, *114*, 1089–1107.

Macedo, J. M., & Marshak, S. (1999). Controls on the geometry of fold-thrust belt salient. *Geological Society of America Bulletin*, *111*(12), 1808–1822. https://doi.org/10.1130/0016-7606(1999)111%3C1808:COTGOF%3E2.3.CO;2

Maesano, F. E., & D'Ambrogi, C. (2016). Coupling sedimentation and tectonic control: Pleistocene evolution of the central Po Basin. *Italian Journal of Geosciences*, *135*(3), 394–407. https://doi.org/10.3301/IJG.2015.17

Maesano, F. E., & D'Ambrogi, C. (2017). Vel-IO 3D: A tool for 3D velocity model construction, optimization and time-depth conversion in 3D geological modeling workflow. *Computers & Geosciences*, *99*, 171–182. https://doi.org/10.1016/j.cageo.2016.11.013

Maesano, F. E., D'Ambrogi, C., Burrato, P., & Toscani, G. (2015). Slip-rates of blind thrusts in slow deforming areas: Examples from the Po Plain (Italy). *Tectonophysics*, *643*, 8–25. https://doi.org/10.1016/j.tecto.2014.12.007

Malagnini, L., Herrmann, R. B., Munafò, I., Buttinelli, M., Anselmi, M., Akinci, A., & Boschi, E. (2012). The 2012 Ferrara seismic sequence: Regional crustal structure, earthquake sources, and seismic hazard. *Geophysical Research Letters*, *39*, L19302. https://doi.org/10.1029/2012GL053214

Malekzade, Z., Bellier, O., Abbassi, M. R., Shabanian, E., & Authemayou, C. (2016). The effects of plate margin inhomogeneity on the defor mation pattern within west-Central Zagros Fold-and-Thrust Belt. *Tectonophysics*, *693*, 304–326. https://doi.org/10.1016/j.tecto.2016.01.030

Malinverno, A., & Ryan, W. B. F. (1986). Extension in the Tyrrhenian Sea and shortening in the Apennines as a result of arc migration driven by sinking of the lithosphere. *Tectonics*, *5*, 227–245. https://doi.org/10.1029/TC005i002p00227

Mariotti, G., & Doglioni, C. (2000). The dip of the foreland monocline in the Alps and Apennines. *Earth and Planetary Science Letters*, *181*(1-2), 191–202. https://doi.org/10.1016/S0012-821X(00)00192-8

Marshak, S. (1988). Kinematics of orocline and arc formation in thin-skinned orogens. *Tectonics*, *7*, 73–86. https://doi.org/10.1029/TC007i001p00073

Marshak, S. (2004). Salients, recesses, arcs, oroclines, and syntaxes—A review of ideas concerning the formation of map-view curves in fold thrust belts. In K. R. McClay (Ed.), *Thrust tectonics and hydrocarbon systems*, *Memoir* (Vol. 82, pp. 131–156). Tulsa, OK: American Association of Petroleum Geologists.

Masetti, D., Fantoni, R., Romano, R., Sartorio, D., & Trevisani, E. (2012). Tectonostratigraphic evolution of the Jurassic extensional basins of the eastern southern Alps and Adriatic foreland based on an integrated study of surface and subsurface data. *AAPG Bulletin*, *96*(11), 2065–2089. https://doi.org/10.1306/03091211087

Massoli, D., Koyi, H. A., & Barchi, M. R. (2006). Structural evolution of a fold and thrust belt generated by multiple décollements: Analogue models and natural examples from the Northern Apennines (Italy). *Journal of Structural Geology*, *28*(2), 185–199. https://doi.org/10.1016/j.jsg.2005.11.002

Merle, O. (1989). Strain models within spreading nappes. *Tectonophysics*, *165*(1-4), 57–71. https://doi.org/10.1016/0040-1951(89)90035-8

Michetti, M., Giardina, F., Livio, F., Mueller, K., Serva, L., Sileo, G., et al. (2012). Active compressional tectonics, Quaternary capable faults, and the seismic landscape of the Po Plain (northern Italy). *Annals of Geophysics*, *55*(5), 969–1001. https://doi.org/10.4401/ag-5462

Miser, H. D. (1932). Oklahoma structural salient of the Ouachita Mountains. *Geological Society of America Bulletin*, *43*, 138.

Mitra, G. (1997). Evolution of salients in a fold-and-thrust belt: The effects of sedimentary basin geometry, strain distribution and critical taper. In I. S. Sengupta (Ed.), *Evolution of Geological Structures in Micro- to Macroscales* (pp. 59–90). London: Chapman and Hall. https://doi.org/10.1007/978-94-011-5870-1_5

Molinari, I., Argnani, A., Morelli, A., & Basini, P. (2015). Development and testing of a 3D seismic velocity model of the Po Plain sedimentary basin, Italy. *Bulletin of the Seismological Society of America*, *105*(2A), 753–764. https://doi.org/10.1785/0120140204

Molli, G., & Meccheri, M. (2012). Structural inheritance and style of reactivation at mid-crustal levels: A case study from the Alpi Apuane (Tuscany, Italy). *Tectonophysics*, *579*, 74–87. https://doi.org/10.1016/j.tecto.2012.06.044

Molli, G., Torelli, L., & Storti, F. (2016). The 2013 Lunigiana (Central Italy) earthquake: Seismic source analysis from DInSar and seismological data, and geodynamic implications for the northern Apennines. A discussion. *Tectonophysics*, *668*, 108–112.

Mouthereau, F., Deffontaines, B., Lacombe, O., & Angelier, J. (2002). Along-strike variations of the Taiwan belt front: Basement control on structural style, wedge geometry and kinematics. *Geological Society of America Special Publication*, *358*(3), 35–58.

Ori, G. G., & Friend, P. F. (1984). Sedimentary basins formed and carried piggyback on active thrust sheets. *Geology*, *12*(8), 475–478. https://doi.org/10.1130/0091-7613(1984)12%3C475:SBFACP%3E2.0.CO;2

Patacca, E., Sartori, R., & Scandone, P. (1992). Tyrrhenian basin and Apenninic arcs: Kinematic relations since Late Tortonian times. *Memorie della Societa Geologica Italiana*, *45*, 425–451.

Perrin, C., Manighetti, I., & Gaudemer, Y. (2016). Off-fault tip splay networks: A genetic and generic property of faults indicative of their long term propagation. *Comptes Rendus Geoscience*, *348*(1), 52–60. https://doi.org/10.1016/j.crte.2015.05.002

Picotti, V., Capozzi, R., Bertozzi, G., Mosca, F., Sitta, A., & Tornaghi, M. (2007). The Miocene petroleum system of the Northern Apennines in the central Po Plain (Italy). In O. Lacombe, J. Lavé, F. Roure, & J. Vergés (Eds.), *Thrust belts and foreland basins. From fold Kinematics to Hydrocarbon Systems* (pp. 117–131). Berlin: Springer. https://doi.org/10.1007/978-3-540-69426-7_6

Picotti, V., & Pazzaglia, F. J. (2008). A new active tectonic model for the construction of the Northern Apennines mountain front near Bologna (Italy). *Journal of Geophysical Research*, *113*, B08412. https://doi.org/10.1029/2007JB005307

Pieri, M. (1983). Three seismic profiles through the Po Plain, in Seismic Expression of Structural Stiles. In A.W Bally (Ed.), American Association of Petroleum Geologists. *Studies in Geology*, *15*(3.4.1), 8–26.

Pieri, M., & Groppi, G. (1981). *Subsurface geological structure of the Po Plain*, *Italy*, *Progetto finalizzato Geodinamica- Sottoprogetto 5- Modello strutturale* (Publ. 414). Roma: CNR.

Pola, M., Ricciato, A., Fantoni, R., Fabbri, P., & Zampieri, D. (2014). Architecture of the western margin of the North Adriatic foreland: The Schio Vicenza fault system. *Italian Journal of Geosciences*, *133*(2), 223–234. https://doi.org/10.3301/IJG.2014.04

Ravaglia, A., Seno, S., Toscani, G., & Fantoni, R. (2006). Mesozoic extension controlling the Southern Alps thrust front geometry under the Po Plain, Italy: insights from sandbox models, in Tectonic Inversion and Structural Inheritance in Mountain Belts. In R.W.H. Butler, E. Tavarnelli, and M. Grasso (Eds.). *Journal of Structural Geology Special Publication*, *28*(11), 2084–2096. https://doi.org/10.1016/j.jsg.2006.07.011

Ricci Lucchi, F. (1986). *The foreland basin system of the northern Apennines and related clastic wedges: A preliminary outline*. *Giornale di Geologia, 48*(1–2), 165–186.

Ries, A. C., & Shackleton, R. M. (1976). Arcuate fold belts. *Philosophical transactions of the Royal Society of London, Series A. Mathematical and Physical Sciences*, *283*(1312), 281–288. https://doi.org/10.1098/rsta.1976.0085

Riguzzi, F., Crespi, M., Devoti, R., Doglioni, C., Pietrantonio, G., & Pisani, A. R. (2012). Geodetic strain rate and earthquake size: New clues for seismic hazard studies. *Physics of the Earth and Planetary Interiors*, *206-207*, 67–75. https://doi.org/10.1016/j.pepi.2012.07.005

Rogers, H. D. (1858). *The Geology of Pennsylvania, a government survey* (Vol. 2, p. 1045). Philadelphia: Lippincott.

Rogledi, S. (2010). Assetto strutturale delle unità alpine nella pianura tra il lago d'Iseo e il Garda. Workshop "Rischio sismico nella Pianura Padana," Brescia, 24 November 2010. Retrived from http://cesia.ing.unibs.it/index.php/it/eventi/giornate-distudio/119

Rosenbaum, G., Lister, G. S., & Duboz, C. (2004). The Mesozoic and Cenozoic motion of Adria (central Mediterranean): Constraints and lim itations. *Geodinamica Acta*, *17*(2), 125–139. https://doi.org/10.3166/ga.17.125-139

Royden, L. E., Patacca, E., & Scandone, P. (1987). Segmentation and configuration of subducted lithosphere in Italy: An important control on thrust-belt and foredeep-basin evolution. *Geology*, *15*(8), 714–717. https://doi.org/10.1130/0091-7613(1987)15%3C714:SACOSL%3E2.0.CO;2

Rudolph, K. W., Schlager, W., & Biddle, K. T. (1989). Seismic models of a carbonate foreslope-to-basin transition, Picco di Vallandro, Dolomite Alps, northern Italy. *Geology*, *17*(5), 453–456. https://doi.org/10.1130/0091-7613(1989)017%3C0453:SMOACF%3E2.3.CO;2

Ruh, J. B., Gerya, T., & Burg, J. P. (2013). High-resolution 3D numerical modeling of thrust wedges: Influence of décollement strength on transfer zones. *Geochemistry, Geophysics, Geosystems*, *14*, 1131–1155. https://doi.org/10.1002/ggge.20085

Ruh, J. B., Gerya, T., & Burg, J. P. (2017). Toward 4D modeling of orogenic belts: Example from the transpressive Zagros Fold Belt. *Tectonophysics*, *702*, 82–89. https://doi.org/10.1016/j.tecto.2015.09.035

Sacchi, R., & Cadoppi, P. (1988). Oroclines and pseudo-orocline. *Tectonophysics*, *146*(1-4), 47–58. https://doi.org/10.1016/0040-1951(88)90080-7

Scrocca, D., Carminati, E., Doglioni, C., & Marcantoni, D. (2007). Slab retreat and active shortening along the central-northern Apennines. In O. Lacombe, J. Lav, F. Roure, & J. Vergs (Eds.), *Thrust Belts and Foreland Basins: From Fold Kinematics to Hydrocarbon Systems*, *Frontiers in Earth Sciences* (pp. 471–487). Berlin: Springer. https://doi.org/10.1007/978-3-540-69426-7_25

Stafleu, J. A. N., & Schlager, W. (1993). Pseudo-toplap in seismic models of the Schlern-Raibl contact (Sella platform, northern Italy). *Basin Research*, *5*(1), 55–65. https://doi.org/10.1111/j.1365-2117.1993.tb00056.x

Talbot, C. J., & Alavi, M. (1996). The past of a future syntaxis across the Zagros. *Geological Society of London, Special Publication*, *100*(1), 89–109. https://doi.org/10.1144/GSL.SP.1996.100.01.08

Tizzani, P., Castaldo, R., Solaro, G., Pepe, S., Bonano, M., Casu, F., et al. (2013). New insights into the 2012 Emilia (Italy) seismic sequence through advanced numerical modeling of ground deformation InSAR measurements. *Geophysical Research Letters*, *40*, 1971–1977. https://doi.org/10.1002/grl.50290

Toscani, G., Bonini, L., Ahmad, M. I., Di Bucci, D., Di Giulio, A., Seno, S., & Galuppo, C. (2014). Opposite verging chains sharing the same foreland: Kinematics and interactions through analogue models (Central Po Plain, Italy). *Tectonophysics*, *633*, 268–282. https://doi.org/10.1016/j.tecto.2014.07.019

Toscani, G., Burrato, P., Di Bucci, D., Seno, S., & Valensise, G. (2009). Plio-Quaternary tectonic evolution of the northern Apennines thrust fronts (Bologna–Ferrara section, Italy): Seismotectonic implications. *Italian Journal of Geosciences*, *128*, 605–613. https://doi.org/10.3301/IJG.2009.128.2.605

Toscani, G., Seno, S., Fantoni, R., & Rogledi, S. (2006). Geometry and timing of deformation inside a structural arc; the case of the western Emilian folds (Northern Apennine front, Italy). *Bollettino della Societa Geologica Italiana*, *125*(1), 59–65.

Turrini, C., Angeloni, P., Lacombe, O., Ponton, M., & Roure, F. (2015). 3D seismotectonics in the Po Valley basin, Northern Italy. *Tectonophysics*, *661*, 156–179. https://doi.org/10.1016/j.tecto.2015.08.033

Turrini, C., Lacombe, O., & Roure, F. (2014). Present-day 3D structural architecture of the Pô Valley basin, northern Italy. *Marine and Petroleum Geology*, *56*, 266–289. https://doi.org/10.1016/j.marpetgeo.2014.02.006

Turrini, C., Toscani, G., Lacombe, O., & Roure, F. (2016). Influence of structural inheritance on foreland-foredeep system evolution: An example from the Po Valley region (northern Italy). *Marine and Petroleum Geology*, *77*, 376–398. https://doi.org/10.1016/j.marpetgeo.2016.06.022

Vannoli, P., Burrato, P., & Valensise, G. (2015). The Seismotectonics of the Po Plain (Northern Italy): Tectonic diversity in a blind faulting domain. *Pure and Applied Geophysics*, *172*(5), 1105–1142. https://doi.org/10.1007/s00024-014-0873-0

ViDEPI Project (2015). Visibility of petroleum exploration data in Italy. Ministry of Economic Development, National Mining Office for Hydrocarbons and Earth Resources - UNMIG. Retrieved from http://unmig.sviluppoeconomico.gov.it/videpi/videpi.asp

Weil, A. B., & Sussman, A. (2004). Classification of curved orogens based on the timing relationships between structural development and vertical-axis rotations. In A. J. Sussman, & A. B. Weil (Eds.), *Orogenic Curvature: Integrating Paleomagnetic and Structural Analyses Geological Society of America, Special Paper, 383*, 1–17. https://doi.org/10.1130/0-8137-2383-3(2004)383%5B1:CCOBOT%5D2.0.CO;2

Wilson, L. F., Pazzaglia, F. J., & Anastasio, D. J. (2009). A fluvial record of active fault-propagation folding, Salsomaggiore anticline, northern Apennines. *Italy*. *Journal of Geophysical Research*, *114*, B08403. https://doi.org/10.1029/2008JB005984

Yonkee, A., & Weil, A. B. (2010). Reconstructing the kinematic evolution of curved mountain belts: Internal strain patterns in the Wyoming salient, Sevier thrust belt, USA. *Geological Society of America Bulletin*, *122*(1–2), 24–49. https://doi.org/10.1130/B26484.1

Zappaterra, E. (1990). Carbonate paleogeographic sequences of the Periadriatic region. *Bollettino della Societa Geologica Italiana*, *109*, 5–20.